HHS Public Access
Author manuscript
Acc Chem Res. Author manuscript; available in PMC 2022 August 10.

Published in final edited form as:
Acc Chem Res. 2022 March 15; 55(6): 904–915. doi:10.1021/acs.accounts.2c00003.

Advancing Chelation Strategies for Large Metal Ions for Nuclear Medicine Applications

Aohan Hu,
Justin J. Wilson
Department of Chemistry and Chemical Biology, Cornell University, Ithaca, New York 14853, United States

CONSPECTUS

Nuclear medicine leverages radioisotopes of a wide range of elements, a significant portion of which are metals, for the diagnosis and treatment of disease. To optimally use the radioisotopes of the metal ions, or radiometals, for these applications, a chelator that efficiently forms thermodynamically and kinetically stable complexes with them is required. The chelator also serves a role of attaching to a biological targeting vector that locates pathological tissues. Numerous chelators suitable for small radiometals have been established to date, but chelators that work well for large radiometals are significantly less common. In this Account, we describe recent progress by us and others in the advancement of ligands for large radiometals chelation with arising applications in nuclear medicine.

First, we discuss and analyze the coordination chemistry of the chelator macropa, a macrocyclic ligand that contains the 18-crown-6 backbone and two picolinate pendent arms, with large metal ions in the context of nuclear medicine. This ligand is known for its unusual reverse size selectivity, or preference for binding large over small metal ions. The radiolabeling properties of macropa with the large radiometals $^{225}Ac^{3+}$, $^{132/135}La^{3+}$, $^{131}Ba^{2+}$, $^{223}Ra^{2+}$, $^{213}Bi^{3+}$, and the related in vivo investigations are described. The development of macropa derivatives containing different pendent donors or rigidifying groups in the macrocyclic core is also briefly reviewed.

Next, efforts towards transforming macropa into a radiopharmaceutical agent via covalent conjugation to biological targeting vectors are summarized. In this discussion, two different types of bifunctional analogues of macropa reported in the literature, macropa-NCS and mcp-click, are presented. Their implementation in different radiopharmaceutical agents is discussed. Bioconjugates containing macropa attached to small-molecule targeting vectors or macromolecular antibodies are presented. The in vitro and in vivo evaluation of these constructs is also discussed.

Lastly, chelators with a dual size selectivity are described. This class of ligands exhibits good affinities to both the large and small metal ions. This property is valuable for nuclear medicine applications that require the simultaneous chelation of both large and small radiometals with complementary therapeutic and diagnostic properties. Recently, we reported an 18-membered

Corresponding Author: Justin J. Wilson – Department of Chemistry and Chemical Biology, Cornell University, Ithaca, New York 14853, United States; jjw275@cornell.edu.

The authors declare no competing financial interest.

macrocyclic ligand called macrodipa that attains this selectivity pattern. This chelator, its second generation analogue py-macrodipa, and their applications for chelating the medicinally relevant large $^{135}La^{3+}$, $^{225}Ac^{3+}$, $^{213}Bi^{3+}$ and small $^{44}Sc^{3+}$ ions are also presented. Studies with these radiometals show that py-macrodipa can effectively radiolabel and stably retain both small and large radiometals. Overall, this Account makes the case for innovative ligand design approaches to employ novel arising radiometal ions with unusual coordination chemistry properties.

Graphical Abstract

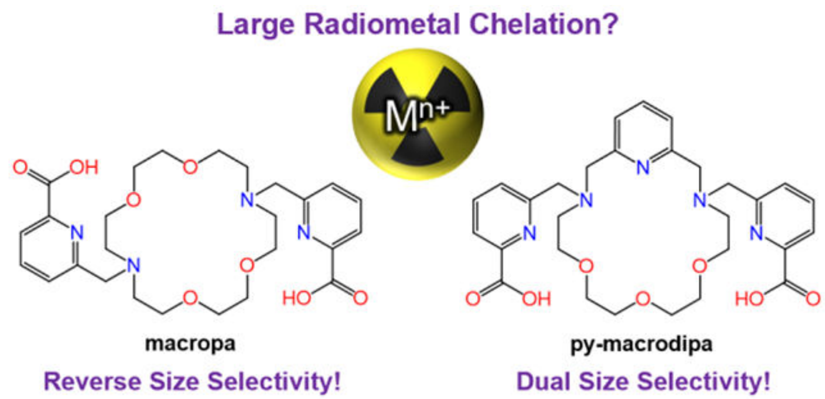

1. Introduction

Nuclear medicine is an important branch of radiology that uses ionizing radiation to treat and diagnose diseases. An area of this field that has attracted significant attention within the last two decades is the implementation of internally administered radionuclides in the form of radiopharmaceutical agents.[5–8] Radionuclides that undergo radioactive decay via positron emission, electron capture, or internal conversion, are leveraged for diagnostic applications within positron emission tomography (PET) and single-photon emission computed tomography (SPECT). By contrast, radionuclides that emit α particles, β^- particles, or Auger electrons, are used for therapy. Elements with radioisotopes suitable for nuclear medicine span nearly the entire periodic table.[9–12] In recent years, the diagnostic and therapeutic potential of large radiometals that reside at the bottom of the periodic table (the fifth period and below), have been recognized. There have been significant efforts to harness them for these applications, as summarized in Table 1.

To transform radiometals into useful therapeutic or diagnostic agents, a chelator is usually required. The chelator serves a critical role in preventing toxicity from the free ions by forming stable metal complexes. These chelators also need to be linked to biological targeting vectors, which selectively target pathological cells. For nuclear medicine, an ideal chelator should address two major challenges. First, it should rapidly incorporate the desired radiometal under mild conditions. Radioactive decay of the radiometal occurs continuously during the radiolabeling process, thereby leading to diminished radiochemical yields if this process is slow. Furthermore, some biological targeting vectors, like antibodies, are only stable near physiological pH and below 37 °C, thus necessitating these conditions for radiolabeling. The second criterion is that they form complexes of sufficient thermodynamic and kinetic stability to prevent in vivo radiometal release.[23] Although the kinetic stability is challenging to directly quantify, the thermodynamic stability of a metal–ligand coordination complex is readily measured by its stability constant, K_{ML}. This constant provides a useful quantitative metric for chelator design efforts.[24] The K_{ML} is defined in eq 1, where [M], [L], and [ML] represent the concentrations of the free metal ions, fully deprotonated ligand, and metal–ligand complex at chemical equilibrium. This constant is pH-independent.

$$K_{ML} = [ML]/[M][L] \quad (1)$$

However, the inherent competition between metal binding and protonation of a ligand must be considered in assessing thermodynamic stability. Thus, the ligand basicity, which will affect the conditional stability constant at physiological pH, is another factor that should be considered in these design efforts. For simplicity, our discussions will focus primarily on K_{ML} values, as a sufficient comparator for trends in metal ion selectivity patterns.

To date, nearly all chelators used in clinically approved metal-based radiopharmaceutical agents are derivatives of 1,4,7,10-tetraazacyclododecane-1,4,7,10-tetraacetic acid (DOTA, Chart 1)[25] and diethylenetriaminepentaacetic acid (DTPA, Chart 1). Despite the success of these ligands with smaller ions, like Lu^{3+} and In^{3+}, they are significantly less effective for the medicinally valuable large radiometals collected in Table 1. Even though vast research efforts have been devoted to chelator development for nuclear medicine,[11,12,23,26] the majority of these candidates are unsuitable for large radiometals. The scarcity of chelators for large metal ions highlights the inherent challenges associated with their coordination chemistry. Specifically, the smaller charge densities of large ions weaken their electrostatic interactions with ligands, and their large sizes require unusual ligands that provide a large coordination cavity and multiple donor atoms. Given the great diagnostic and therapeutic potential of these large radiometals, novel chelation strategies are necessary to effectively harness them.

2. Chelating Large Metal Ions with Macropa

Towards identifying and designing effective chelators for large metal ions, researchers often investigate their coordination chemistry with the rare-earth ions (Ln^{3+}, Figure 1). All 17 Ln^{3+} ions have similar chemical properties with respect to their oxidation states and ligand donor atom preferences. The only distinguishing feature is their ionic radii, which range from 103.2 pm for La^{3+} to 74.5 pm for Sc^{3+}.[27,28] Thus, this class of elements provides a straightforward means of understanding the size-selectivity of a chelator. Furthermore, a number of Ln^{3+} ions have valuable medicinal applications.[29] In addition to the rare-earth radionuclides listed in Table 1, $^{149/152/155/161}Tb^{3+}$, $^{86/90}Y^{3+}$, $^{177}Lu^{3+}$, and $^{44/47}Sc^{3+}$ are also relevant to nuclear medicine.[12] Eu^{3+} and Tb^{3+} complexes can be employed as photoluminescent probes,[30] and Gd^{3+} is clinically used in magnetic resonance imaging contrast agents.[31]

Analysis of the K_{ML} values of most chelators for their Ln^{3+} complexes reveals the general trend of a higher affinity for the heavier, smaller Ln^{3+}, which is most likely a consequence of their higher charge density that leads to more pronounced metal–ligand electrostatic interactions.[32] This trend is observed for an overwhelming majority of chelators, including the extensively used DOTA, DTPA, and ethylenediaminetetraacetic acid (EDTA) (Figure 2a). Chelators with a “reverse size selectivity”, which display a higher affinity for large Ln^{3+}, are rare.

Because of recent interest in the large radiometals for nuclear medicine applications, there has been a draw to find chelators that exhibit the reverse size selectivity. Early studies identified chelators based on the 4,13-diaza-18-crown-6 macrocyclic core to possess a preference for large Ln^{3+}. For instance, odda (Chart 2, Figure 2b) shows a greater affinity for large Ln^{3+} ions, albeit with a modest selectivity across the series ($\log K_{CeL} - \log K_{LuL} = 1.4$).[37] Its analogue oddm also prefers large Ln^{3+}, but with a greater selectivity ($\log K_{CeL} - \log K_{LuL} = 5.4$).[40] These studies indicated that the 4,13-diaza-18-crown-6 macrocycle potentially confers this unusual selectivity.

In 2009, the chelator macropa or bp18c6, a derivative of the 4,13-diaza-18-crown-6 macrocycle with two pendent picolinate arms, was also shown to be reverse-size-selective (Figure 2b), with an unprecedented ability to discriminate the large and small Ln^{3+} ($\log K_{CeL} - \log K_{LuL} = 6.9$).[38] Its large Ln^{3+} complexes exhibit both excellent thermodynamic and kinetic stability. The La^{3+}–macropa complex has a $\log K_{LaL} = 14.99$[38] and is kinetically stable for three weeks in the presence of 1000-equivalents of DTPA at pH 7.4.[1] Crystal structures of the La^{3+} and Lu^{3+} macropa complexes (Figure 3a,b) provide insight on the reverse size selectivity of this ligand. Even though both complexes attain a distorted C_2 symmetry, notable disparities in the interatomic distances are found within these two structures. For example, La–N1 and La–N2 distances are 0.04 Å from each other, whereas the Lu–N1 and Lu–N2 distances differ by 0.10 Å, indicating a greater degree of asymmetry for the latter. Furthermore, the 18-crown-6 scaffold in the Lu^{3+} complex is significantly more puckered than in the La^{3+} complex, signifying a higher ligand strain for the former, as also supported by computational studies.[41] These observations indicate that the 4,13-diaza-18-crown-6 macrocyclic backbone is optimally suited for interacting with large ions, like La^{3+}. Other computational studies on macropa metal-binding properties also provided insight on its selectivity by noting a subtle balance between the metal–ligand binding energy and Ln^{3+} hydration energy.[42] Moreover, the reverse size selectivity of macropa extends to other classes of metal ions, such as the alkaline-earths, where the K_{ML} trend follows $K_{BaL} > K_{SrL} > K_{CaL}$.[43,44]

The pronounced reverse size selectivity of macropa prompted us to explore its ability to chelate large radiometals for nuclear medicine applications. Our particular interest when we initiated this project five years ago was the therapeutic α-emitting $^{225}Ac^{3+}$.[16] Its conjugation to appropriate biological targeting vectors required the use of DOTA, necessitating either a two-step radiolabeling process[46] or a long incubation, due to the slow binding kinetics of this ligand.[47] Given the high affinity of macropa for La^{3+} and the chemical similarity of La^{3+} and Ac^{3+},[48] we reasoned that macropa would be an effective chelator for this promising therapeutic radiometal. In line with this expectation, we discovered that macropa quantitatively complexed $^{225}Ac^{3+}$ within 5 min at RT and pH 5.5–6 at sub-μM ligand concentration, surpassing the high-temperature conditions required for DOTA. To evaluate the in vivo stability of the $[^{225}Ac][Ac(macropa)]^+$ complex, we performed biodistribution studies in C57BL/6 mice, using [^{225}Ac]Ac(NO_3)$_3$ as the control. The biodistribution profile of [^{225}Ac]Ac(NO_3)$_3$ shows a slow blood clearance with accumulation occurring in the liver and spleen (Figure 4a). By contrast, [^{225}Ac][Ac(macropa)]$^+$ was rapidly excreted from the mice, giving negligible residual activity in these organs (Figure 4b). This distinction indicates that [^{225}Ac][Ac(macropa)]$^+$ does not release free $^{225}Ac^{3+}$ in vivo.[1] Thus, the rapid radiolabeling kinetics and excellent in vivo stability revealed macropa to be a highly promising chelator for $^{225}Ac^{3+}$ therapy.

We next investigated macropa for medicinally relevant radioisotopes of La^{3+}. In particular, the pair $^{132/135}La^{3+}$ can be used for PET imaging and Auger electron therapy, respectively.[15,49] Like Ac^{3+}, the large ionic radius of La^{3+} makes conventional chelators like DOTA and DTPA poorly effective. In our radiolabeling studies, we found that macropa complexed $^{132/135}La^{3+}$ with a high apparent molar activity (4.34 Ci·μmol^{-1}) at RT and pH 5.5 within 30 min. By contrast, even with an elevated temperature (80 °C), DOTA reached a molar activity of only 0.67 Ci·μmol^{-1}.[50]

$^{223}Ra^{2+}$, another promising large therapeutic radiometal, is currently the only α-particle emitter approved for clinical use in the form of unchelated [^{223}Ra]$RaCl_2$, applied for the management of bone metastases in castration-resistant prostate cancer patients.[51] As the largest divalent cation in the periodic table (8-coordinate ionic radius 148 pm),[28] the identification of suitable chelators for $^{223}Ra^{2+}$ has been significantly hindered. In this context, we established that macropa shows a high affinity for Ba^{2+}, the lighter congener of Ra^{2+}, forming a complex of analogous geometry as that of La^{3+} (Figure 3c). Macropa is thus a potent barite scale dissolution agent, a problem of significance in the petroleum industry.[44] Furthermore, macropa was recently evaluated for chelation of the diagnostic $^{131}Ba^{2+}$ by others. Within an hour, macropa quantitatively radiolabeled $^{131}Ba^{2+}$ at RT and pH 6 at a ligand concentration of 10^{-4} M. The resulting radiometal complex did not dissociate within 3 d after being incubated in human serum at 37 °C.[52]

Thus, we sought to explore macropa as a potential candidate for $^{223}Ra^{2+}$ complexation. Consistent with its Ba^{2+}-binding properties, macropa formed the [^{223}Ra][Ra(macropa)] complex quantitatively within 5 min at RT and pH 6, and the ligand concentration required for 50% radiolabeling efficiency was determined to be 13 mM. Importantly, [^{223}Ra][Ra(macropa)] remained ~90% intact in human serum at 37 °C after 12 d.[3] In vivo mouse studies comparing [^{223}Ra][Ra(macropa)] and [^{223}Ra]$RaCl_2$ revealed distinct biodistribution properties. Consistent with the bone-seeking property of Ra^{2+},[53] [^{223}Ra]$RaCl_2$ accumulated in bone (Figure 5a),whereas the bone uptake of $^{223}Ra^{2+}$ was markedly reduced within mice injected with [^{223}Ra][Ra(macropa)] (Figure 5b). The intestine and spleen uptake were also significantly decreased. These substantial differences suggest that [^{223}Ra][Ra(macropa)] remains intact in vivo.[3]

As the most recent example, we investigated the coordination chemistry of macropa with Bi^{3+} and its suitability for the therapeutic α-emitting $^{213}Bi^{3+}$. Unlike the s- and f-block metal ions discussed above, Bi^{3+} usually forms coordination complexes with anisotropic coordination spheres, due to the stereochemical activity of the $6s^2$ lone pair.[54,55] The crystal structure of [Bi(macropa)]$^+$ is notably different than those of the La^{3+}, Lu^{3+}, and Ba^{2+}

complexes (Figure 3). The Bi^{3+} center sits asymmetrically within the coordination sphere, and the macrocyclic donor atoms do not fully engage with Bi^{3+}, a consequence of the Bi^{3+} $6s^2$ stereochemical activity. In the radiolabeling studies, macropa efficiently complexed ^{213}Bi within 8 min at RT and pH 5.5–6 at a ligand concentration of $\geq 10^{-6}$ M.[45] Collectively, macropa has proven to be an effective chelator for large radiometals including several promising α-emitting radionuclides.

On account of the efficacy of macropa, we and others have been investigating analogues of this ligand. Macropa was altered by either varying the pendent donors (macropaquin, macroquin-SO_3, macrophospho, macrophosphi, Chart 3)[39,44,45,56] or modifying the macrocyclic backbone (CHX-macropa, BZ-macropa, Chart 3).[41,57] Notably, macroquin-SO_3 forms a highly kinetically stable complex with Bi^{3+}, suggesting its promise for $^{213}Bi^{3+}$ chelation.[45] Moreover, macrophosphi retains its reverse size selectivity, but differs from macropa in its pronounced ability to discriminate light Ln^{3+} ions (Figure 2b). This property was leveraged for an effective liquid-liquid extraction separation between the adjacent early Ln^{3+} ions, La^{3+} and Ce^{3+}.[39]

3. Development of Macropa-Based Bifunctional Chelators and Bioconjugates for Radiopharmaceutical Applications

As highlighted above, macropa is an effective chelator for large radiometals with relevance to nuclear medicine. For actual radiopharmaceutical applications, however, they need to be conjugated to biological targeting vectors, like peptides, antibodies, polysaccharides, and lipids, which selectively target pathological locations. For this purpose, bifunctional chelators, which contain both the metal-binding component and a reactive functional group, are needed. This reactive group can form covalent bonds with biomolecules, giving rise to a bioconjugate (Figure 6) that can be directly used in radiopharmaceutical contexts.[5,58]

To take advantage of the effective radiometal-binding properties of macropa, a bifunctional analogue, macropa-NCS (Chart 4a), was prepared via an 8-step organic synthesis.[1] The isothiocyanate group (–NCS), which reacts with a primary amine to form a thiourea linkage,[59] was introduced. Macropa-NCS was then successfully conjugated to a small molecule, giving a bioconjugate RPS-070 (Chart 4b). It contains a “Lys–urea–Glu” moiety, which targets the prostate-specific membrane antigen (PSMA) that is overexpressed in prostate cancer.[60] In addition, a serum-albumin-binding iodophenyl group was also included to prolong in vivo circulation.[61] Like free macropa, RPS-070 rapidly incorporated $^{225}Ac^{3+}$ within 20 min at RT and pH 5–5.5, demonstrating that the newly-introduced biomolecule does not negatively affect the coordination properties of this ligand. Furthermore, the radiometal complex ^{225}Ac–RPS-070 shows significant uptake in the tumors of mice bearing LNCaP (PSMA+ prostate cancer) xenografts with no other apparent off-target accumulation. However, ^{225}Ac–RPS-070 exhibited fast renal clearance as marked by a significant loss the radioactivity within 4 h.[1]

To extend the in vivo circulation of RPS-070, an analogue of this compound, RPS-074 (Chart 4b), was prepared by modifying the length of the PEG-linking units between macropa, the PSMA-targeting moiety, and the albumin-binding iodophenyl group. Like macropa and RPS-070, RPS-074 rapidly binds to and forms a stable complex with $^{225}Ac^{3+}$. In contrast to ^{225}Ac–RPS-070, the circulation of ^{225}Ac–RPS-074 is significantly longer, resulting in a larger and more prolonged accumulation in the LNCaP prostate tumor xenografts in mice (Figure 7a). Although a clear dose-response was not apparent in these studies due to challenges with tumor size heterogeneity, all administered doses at the beginning of a 75-day therapy study resulted in significantly retarded tumor growth, and an increased survival of mice over the experiment duration compared to the vehicle-treated control (Figure 7b).[62]

Macropa-NCS was also conjugated to the monoclonal antibody, trastuzumab, and the resulting antibody-chelator construct was labeled with $^{225}Ac^{3+}$.[1] In subsequent work by others, macropa-NCS was attached to the humanized monoclonal IgG1 antibody GC33,[63] which binds to the protein glypican-3 that is highly expressed in liver cancer.[64] Like the macropa-trastuzumab conjugate, macropa-GC33 was effective at complexing and retaining ^{225}Ac, as >95% of it remained intact after being incubated in human serum for 14 d at 37 °C. ^{225}Ac–macropa-GC33 was further evaluated in mice bearing liver cancer HepG2 tumor xenografts. Its biodistribution revealed substantial tumor uptake (12.9 %ID·g^{-1} at 48 h and 12.0 %ID·g^{-1} at 144 h post injection), consistent with the liver-cancer-targeting property of GC33. Furthermore, ^{225}Ac–macropa-GC33 was able to prolong the survival of these mice compared to the untreated control, providing further support for the use of macropa in radiopharmaceutical therapy.[63]

We also applied macropa-NCS with a smaller PSMA-targeting moiety called DUPA to assess this bifunctional chelator for $^{132/135}La^{3+}$ and $^{223}Ra^{2+}$. This bioconjugate, macropa-DUPA (Chart 4b), was tested with $^{132/135}La^{3+}$, revealing quantitative radiolabeling within 30 min at RT and pH 5.5. $^{132/135}$La–macropa-DUPA was then assessed in mice bearing two implanted tumor xenografts, comprising PSMA+ (PC3-PIP) and PSMA− (PC3-flu) cells. PET/CT scans on these mice revealed significant uptake of the radiotracer only in the PSMA+ xenograft both 1 and 4 h post-injection (Figure 8), and this result was further verified by ex vivo biodistribution studies.[50] This study signified the first example of employing La^{3+} radioisotopes for radiopharmaceutical imaging.

Subsequently, we evaluated macropa-DUPA with $^{223}Ra^{2+}$. Consistent with studies on the unfunctionalized macropa, macropa-DUPA efficiently incorporated $^{223}Ra^{2+}$, and the resulting complex remained >90% intact after 12 d in human serum at 37 °C. However, the biodistribution of ^{223}Ra–macropa-DUPA revealed significant bone uptake matching that of [^{223}Ra]$RaCl_2$, suggesting that ^{223}Ra–macropa-DUPA is unstable in vivo, in stark contrast to the in vivo stability observed for [$^{223}Ra^{2+}$][Ra(macropa)].[3] These observations highlight an important but scarcely understood phenomenon; the biological targeting vector can have a profound effect on complex stability.

Despite the value of macropa-NCS as a bifunctional chelator, its vulnerability to hydrolysis limits its potential. The electron-withdrawing nature of the picolinate makes the –NCS functional group significantly more reactive. For example, compared to the bifunctional DOTA, *p*-NCS-Bn-DOTA (Chart 4a), which contains the –NCS group on a phenyl group, macropa-NCS undergoes hydrolysis 10-times faster.[1] Thus, the development of alternative, more bench-stable bifunctional analogues of macropa is desirable. In this context, mcp-M-click and mcp-D-click (Chart 4c) were recently reported.[65] The more stable alkyne groups in these ligands can undergo the copper-catalyzed azide-alkyne cycloaddition (CuAAC) click reaction.[59,66] Leveraging this chemistry, these ligands were successfully conjugated to an azide-containing PSMA-targeting peptide, yielding mcp-M-PSMA and mcp-D-PSMA. Both bioconjugates retained excellent radiolabeling efficiencies with $^{225}Ac^{3+}$. In particular, ^{225}Ac–mcp-D-PSMA exhibited high binding affinity to PSMA and effectively inhibited the growth of LNCaP cells in an in vitro colony formation assay. Lastly, biodistribution studies of both bioconjugates in mice bearing LNCaP tumors revealed them to preferentially accumulate in the tumors.[65]

4. Stable Chelation for Both the Large and Small Metal Ions: The “Macrodipa-Type” Chelators and Their Dual Size Selectivity

A key limitation of macropa is its ineffectiveness for smaller radiometal ions. This property is concerning because most metallic radionuclides currently used in nuclear medicine are smaller ions, like the diagnostic radiometals $^{68}Ga^{3+}$, $^{111}In^{3+}$, and $^{44}Sc^{3+}$, which are unamenable to macropa chelation.[67] In situations where large and small radiometals are needed simultaneously, such as for theragnostic purposes, a chelator system that effectively binds both types of metal ions would be valuable. In addition, chelating both large and small ions with a single ligand is more beneficial than using two distinct structures. Two metal complexes arising from the same ligand should have comparable chemical properties that manifest in similar in vivo biodistribution and circulation time, which is critical for theragnostics.

Towards this goal, we reported a macrocyclic chelator macrodipa (Chart 5) that shows an unprecedented “dual size selectivity” for the Ln^{3+} ions. As shown in Figure 9a, macrodipa exhibits better affinities for both the large and small Ln^{3+}.[2] Crystallographic analysis of its La^{3+} and Lu^{3+} complexes (Figure 9b) revealed that macrodipa attains two distinct conformations in binding large ions like La^{3+} and small ions like Lu^{3+}. Upon binding La^{3+}, a 10-coordinate, nearly C_2-symmetric complex forms, in which all six donor atoms on the macrocyclic backbone interact with the metal (Conformation A). By contrast, in the Lu^{3+} structure, three of the oxygen atoms present within the macrocycle do not directly engage with the central ion, resulting in an 8-coordinate, asymmetric complex (Conformation B). In addition to X-ray crystallography, comprehensive NMR spectroscopic studies verified these two distinct conformations in solution. Furthermore, DFT calculations revealed that Conformation A is energetically favored for large ions, whereas B is more stable for small ions. Thus, the unique dual size selectivity of macrodipa arises from its conformational toggle that enables the accommodation of both large and small metal ions.[2]

Despite this novel selectivity pattern, the Ln^{3+} complexes of macrodipa are labile, as reflected by their instability to transchelation by DTPA.[4] This lability precludes the use of macrodipa for nuclear medicine, thus prompting us to pursue alternative but related ligand design strategies. It has been demonstrated that the installation of pyridyl donors, in place of ethereal oxygen donors, augments complex stability. The pyridine-containing pypa, for example, represents an improvement over Oxyaapa (Chart 5).[68,69] Following this lead, we targeted a macrodipa analogue, py-macrodipa (Chart 5), which replaces one of the ethereal oxygen donors with a pyridyl moiety.[4] As plotted in Figure 9a, this modification led to a significant enhancement of the thermodynamic stability of its Ln^{3+} complexes without compromising its dual-size-selectivity profile. Like for macrodipa, a suite of X-ray crystallographic (Figure 10a), NMR spectroscopic, and DFT studies verified that py-macrodipa achieves this selectivity pattern by accommodating both large and small ions in different Conformations A and B. Importantly, the kinetic stability of the Ln^{3+} complexes of py-macrodipa are also considerably greater than those of macrodipa. This enhanced kinetic stability is most likely a consequence of the additional rigidity introduced by the planar pyridyl unit, as well as its stronger donor strength.[4]

Given the enhanced complex stability of py-macrodipa, its potential for nuclear medicine was assessed. To capitalize on its dual size selectivity, two radiometals that represent the maximum and minimum ionic radii within the Ln^{3+} series, $^{135}La^{3+}$ and $^{44}Sc^{3+}$, were chosen. $^{135}La^{3+}$ is a promising Auger electron emitter valuable for therapeutic purposes, whereas $^{44}Sc^{3+}$ is diagnostic positron emitter. The significant size difference of these ions requires different chelators. For example, Sc^{3+} is effectively complexed by DOTA, whereas the corresponding La^{3+} complex is significantly less stable. Likewise, macropa is a good ligand for La^{3+}, but works poorly for Sc^{3+}. Remarkably, py-macrodipa radiolabeled both $^{135}La^{3+}$ and $^{44}Sc^{3+}$, at RT and pH 5.5 within 15 min, with high apparent molar activities. Furthermore, both radiometal complexes were stable in human serum at 37 °C, showing no noticeable dissociation over a timescale that matches their physical half-lives (Figure 10b).[4] These results highlight the effectiveness of py-macrodipa for chelating both the large and small radiometal ions. The clever design strategies applied for py-macrodipa demonstrate the proof-of-principle possibility of developing chelators that can be adopted for radionuclides with disparate ionic radii.

Based on the success of py-macrodipa with $^{135}La^{3+}$ and $^{44}Sc^{3+}$, we next employed this system for other non-Ln^{3+} radiometals, like the large α-emitting radiometals $^{225}Ac^{3+}$ and $^{213}Bi^{3+}$. Despite the nearly identical ionic radii of La^{3+} and Bi^{3+},[28] the Bi^{3+} complex of py-macrodipa adopts the asymmetric Conformation B,[70] which is normally preferred for small ions. This unexpected geometry is possibly a consequence of the stereochemical activity of the Bi^{3+} $6s^2$ lone pair.[54,55] Both $^{225}Ac^{3+}$ and $^{213}Bi^{3+}$ were efficiently incorporated by py-macrodipa at RT and pH 5.5–6, and quantitative radiolabeling was observed for $^{225}Ac^{3+}$ and $^{213}Bi^{3+}$ at ligand concentrations of $\geq 10^{-5}$ and $\geq 10^{-7}$ M, respectively. Even though the py-macrodipa complex with Ac^{3+} is kinetically labile and not optimal for nuclear medicine purposes, the Bi^{3+} complex has a remarkable kinetic stability, surpassing that of macropa.[70] This study established py-macrodipa as a promising candidate for $^{213}Bi^{3+}$ chelation, representing an extension of its versatility for a wide range of metal ions.

5. Conclusions and Outlook

Within recent years, the therapeutic and diagnostic properties of radioisotopes of large metal ions have been recognized for their potential in nuclear medicine. The coordination chemistry of these ions, however, is less developed than those of other more commonly used radionuclides, thus necessitating the advancement of novel chelator systems. In this Account, we have reviewed the efforts from us and others in the last five years towards addressing this challenge.

As we have demonstrated, macropa and its bifunctional analogues have a high promise for chelating large ions, showing significant advantages over the prior state-of-the-art ligand DOTA. In addition, modifying the 18-membered macrocycle affords a new class of macrodipa-type chelators exhibiting a dual size selectivity, which may be valuable for theragnostic applications. Understanding fundamental coordination chemistry and applying that knowledge for clever ligand design approaches are critical in this regard.

There are still significant challenges that will require more efforts in this area. For example, the successful targeting of $^{223}Ra^{2+}$ to tumors has not yet been demonstrated. We also envision that expanding the dual size selectivity concept to specifically match the ionic radii of desired theragnostic radionuclide pairs will be of significant clinical interest and value. Inorganic and coordination chemists have a unique skill set to make key advances in the field of nuclear medicine.

Acknowledgement.

We acknowledge financial support from the National Institutes of Biomedical Imaging and Bioengineering of the National Institutes of Health (Award Numbers R21EB027282, R01EB029259), and the Research Corporation for Science Advancement through a Cottrell Research Scholar Award to J.J.W.

Biographies

Aohan Hu is a Ph.D. candidate in the Department of Chemistry and Chemical Biology at Cornell University. He grew up in Yueyang, Hunan, China and received his B.S. in Chemistry from Wuhan University (2017). His current research is focused on chelator design for heavy metal ions and the medicinal applications of their coordination compounds.

Justin J. Wilson is an associate professor in the Department of Chemistry and Chemical Biology at Cornell University, which he joined in 2015. His research program, which has been recognized by a number of awards including the 2019 Cottrell Scholar Award and the 2022 Harry Gray Award for Creative Work in Inorganic Chemistry by a Young Investigator, is broadly directed toward the development of coordination chemistry for biomedical applications.

REFERENCES

(1). Thiele NA; Brown V; Kelly JM; Amor-Coarasa A; Jermilova U; MacMillan SN; Nikolopoulou A; Ponnala S; Ramogida CF; Robertson AKH; Rodríguez-Rodríguez C; Schaffer P; Williams C Jr.; Babich JW; Radchenko V; Wilson JJ An Eighteen-Membered Macrocyclic Ligand for Actinium-225 Targeted Alpha Therapy. Angew. Chem., Int. Ed 2017, 56, 14712–14717.

(2). Hu A; MacMillan SN; Wilson JJ Macrocyclic Ligands with an Unprecedented Size-Selectivity Pattern for the Lanthanide Ions. J. Am. Chem. Soc 2020, 142, 13500–13506. [PubMed: 32697907]

(3). Abou DS; Thiele NA; Gutsche NT; Villmer A; Zhang H; Woods JJ; Baidoo KE; Escorcia FE; Wilson JJ; Thorek DLJ Towards the Stable Chelation of Radium for Biomedical Applications with an 18-Membered Macrocyclic Ligand. Chem. Sci 2021, 12, 3733–3742. [PubMed: 34163647]

(4). Hu A; Aluicio-Sarduy E; Brown V; MacMillan SN; Becker KV; Barnhart TE; Radchenko V; Ramogida CF; Engle JW; Wilson JJ Py-Macrodipa: A Janus Chelator Capable of Binding Medicinally Relevant Rare-Earth Radiometals of Disparate Sizes. J. Am. Chem. Soc 2021, 143, 10429–10440. [PubMed: 34190542]

(5). Radiopharmaceutical Chemistry; Lewis JS, Windhorst AD, Zeglis BM, Eds.; Springer Nature Switzerland AG: Cham, Switzerland, 2019.

(6). Sgouros G; Bodei L; McDevitt MR; Nedrow JR Radiopharmaceutical Therapy in Cancer: Clinical Advances and Challenges. Nat. Rev. Drug Discovery 2020, 19, 589–608. [PubMed: 32728208]

(7). Dondi M; Kashyap R; Paez D; Pascual T; Zaknun J; Mut Bastos F; Pynda Y Trends in Nuclear Medicine in Developing Countries. J. Nucl. Med 2011, 52, 16S–23S. [PubMed: 22144549]

(8). Delbeke D; Segall GM Status of and Trends in Nuclear Medicine in the United States. J. Nucl. Med 2011, 52, 24S–28S. [PubMed: 22144551]

(9). Blower PJ A Nuclear Chocolate Box: the Periodic Table of Nuclear Medicine. Dalton Trans. 2015, 44, 4819–4844. [PubMed: 25406520]

(10). Cutler CS; Hennkens HM; Sisay N; Huclier-Markai S; Jurisson SS Radiometals for Combined Imaging and Therapy. Chem. Rev 2013, 113, 858–883. [PubMed: 23198879]

(11). Boros E; Packard AB Radioactive Transition Metals for Imaging and Therapy. Chem. Rev 2019, 119, 870–901. [PubMed: 30299088]

(12). Kostelnik TI; Orvig C Radioactive Main Group and Rare Earth Metals for Imaging and Therapy. Chem. Rev 2019, 119, 902–956. [PubMed: 30379537]

(13). Aluicio-Sarduy E; Barnhart TE; Weichert J; Hernandez R; Engle JW Cyclotron-Produced 132La as a PET Imaging Surrogate for Therapeutic ^{225}Ac. J. Nucl. Med 2021, 62, 1012–1015. [PubMed: 33127622]

(14). Bailey TA; Mocko V; Shield KM; An DD; Akin AC; Birnbaum ER; Brugh M; Cooley JC; Engle JW; Fassbender ME; Gauny SS; Lakes AL; Nortier FM; O'Brien EM; Thiemann SL; White FD; Vermeulen C; Kozimor SA; Abergel RJ Developing the ^{134}Ce and ^{134}La Pair as Companion Positron Emission Tomography Diagnostic Isotopes for ^{225}Ac and ^{227}Th Radiotherapeutics. Nat. Chem 2021, 13, 284–289. [PubMed: 33318671]

(15). Fonslet J; Lee BQ; Tran TA; Siragusa M; Jensen M; Kibédi T; Stuchbery AE; Severin GW ^{135}La as an Auger-Electron Emitter for Targeted Internal Radiotherapy. Phys. Med. Biol 2018, 63, 015026.

(16). Geerlings MW; Kaspersen FM; Apostolidis C; van der Hout R The Feasibility of 225Ac as a Source of α-Particles in Radioimmunotherapy. Nucl. Med. Commun 1993, 14, 121–125. [PubMed: 8429990]

(17). Hassfjell S; Brechbiel MW The Development of the α-Particle Emitting Radionuclides ^{212}Bi and ^{213}Bi, and Their Decay Chain Related Radionuclides, for Therapeutic Applications. Chem. Rev 2001, 101, 2019–2036. [PubMed: 11710239]

(18). Reissig F; Kopka K; Mamat C The Impact of Barium Isotopes in Radiopharmacy and Nuclear Medicine – From Past to Presence. Nucl. Med. Biol 2021, 98, 59–68. [PubMed: 34051648]

(19). Marques IA; Neves AR; Abrantes AM; Pires AS; Tavares-da-Silva E; Figueiredo A; Botelho MF Targeted Alpha Therapy Using Radium-223: From Physics to Biological Effects. Cancer Treat. Rev 2018, 68, 47–54. [PubMed: 29859504]

(20). Yong K; Brechbiel M Application of ^{212}Pb for Targeted α-particle Therapy (TAT): Pre-clinical and Mechanistic Understanding through to Clinical Translation. AIMS Med. Sci 2015, 2, 228–245. [PubMed: 26858987]

(21). Frantellizzi V; Cosma L; Brunotti G; Pani A; Spanu A; Nuvoli S; De Cristofaro F; Civitelli L; De Vincentis G Targeted Alpha Therapy with Thorium-227. Cancer Biother. Radiopharm 2020, 35, 437–445. [PubMed: 31967907]

(22). Morgenstern A; Lebeda O; Stursa J; Bruchertseifer F; Capote R; McGinley J; Rasmussen G; Sin M; Zielinska B; Apostolidis C Production of ^{230}U/^{226}Th for Targeted Alpha Therapy via Proton Irradiation of ^{231}Pa. Anal. Chem 2008, 80, 8763–8770. [PubMed: 18925748]

(23). Price EW; Orvig C Matching Chelators to Radiometals for Radiopharmaceuticals. Chem. Soc. Rev 2014, 43, 260–290. [PubMed: 24173525]

(24). Martell AE; Hancock RD Metal Complexes in Aqueous Solutions; Plenum Press: New York, 1996.

(25). Stasiuk GJ; Long NJ The Ubiquitous DOTA and its Derivatives: the Impact of 1,4,7,10-Tetraazacyclododecane-1,4,7,10-tetraacetic Acid on Biomedical Imaging. Chem. Commun 2013, 49, 2732–2746.

(26). Jackson JA; Hungnes IN; Ma MT; Rivas C Bioconjugates of Chelators with Peptides and Proteins in Nuclear Medicine: Historical Importance, Current Innovations, and Future Challenges. Bioconjugate Chem. 2020, 31, 483–491.

(27). Cotton SA Scandium, Yttrium & the Lanthanides: Inorganic & Coordination Chemistry. Encyclopedia of Inorganic Chemistry; John Wiley & Sons, Ltd.: Chichester, UK, 2006.

(28). Shannon RD Revised Effective Ionic Radii and Systematic Studies of Interatomic Distances in Halides and Chalcogenides. Acta Crystallogr., Sect. A: Found. Adv 1976, 32, 751–767.

(29). Cheisson T; Schelter EJ Rare Earth Elements: Mendeleev's Bane, Modern Marvels. Science 2019, 363, 489–493. [PubMed: 30705185]

(30). Bünzli J-CG Lanthanide Luminescence for Biomedical Analyses and Imaging. Chem. Rev 2010, 110, 2729–2755. [PubMed: 20151630]

(31). Wahsner J; Gale EM; Rodríguez-Rodríguez A; Caravan P Chemistry of MRI Contrast Agents: Current Challenges and New Frontiers. Chem. Rev 2019, 119, 957–1057. [PubMed: 30350585]

(32). Piguet C; Bünzli J-CG Mono- and Polymetallic Lanthanide-Containing Functional Assemblies: A Field between Tradition and Novelty. Chem. Soc. Rev 1999, 28, 347–358.

(33). Martell AE; Smith RM Critical Stability Constants; Plenum Press: New York, 1974; Vol. 1.

(34). Cacheris WP; Nickle SK; Sherry AD Thermodynamic study of Lanthanide Complexes of 1,4,7-Triazacyclononane-*N,N′,N″*-triacetic Acid and 1,4,7,10-Tetraazacyclododecane-*N,N′,N″,N‴*-tetraacetic Acid. Inorg. Chem 1987, 26, 958–960.

(35). Moeller T; Thompson LC Observations on the Rare Earths—LXXV: The Stabilities of Diethylenetriaminepentaacetic Acid Chelates. J. Inorg. Nucl. Chem 1962, 24, 499–510.

(36). Grimes TS; Nash KL Acid Dissociation Constants and Rare Earth Stability Constants for DTPA. J. Solution Chem 2014, 43, 298–313.

(37). Chang CA; Rowland ME Metal Complex Formation with 1,10-Diaza-4,7,13,16-tetraoxacyclooctadecane-*N,N′*-diacetic Acid. An Approach to Potential Lanthanide Ion Selective Reagents. Inorg. Chem 1983, 22, 3866–3869.

(38). Roca-Sabio A; Mato-Iglesias M; Esteban-Gómez D; Tóth É; de Blas A; Platas-Iglesias C; Rodríguez-Blas T Macrocyclic Receptor Exhibiting Unprecedented Selectivity for Light Lanthanides. J. Am. Chem. Soc 2009, 131, 3331–3341. [PubMed: 19256570]

(39). Thiele NA; Fiszbein DJ; Woods JJ; Wilson JJ Tuning the Separation of Light Lanthanides Using a Reverse-Size Selective Aqueous Complexant. Inorg. Chem 2020, 59, 16522–16530. [PubMed: 33103417]

(40). Brücher E; Györi B; Emri J; Solymosi P; Sztanyik LB; Varga L 1,10-Diaza-4,7,13,16-tetraoxacyclooctadecane-1,10-bis(malonate), a Ligand with High Sr^{2+}/Ca^{2+} and Pb^{2+}/Zn^{2+} Selectivities in Aqueous Solution. J. Chem. Soc., Chem. Commun 1993, 574–575.

(41). Thiele NA; Woods JJ; Wilson JJ Implementing f-Block Metal Ions in Medicine: Tuning the Size Selectivity of Expanded Macrocycles. Inorg. Chem 2019, 58, 10483–10500. [PubMed: 31246017]

(42). Regueiro-Figueroa M; Esteban-Gómez D; de Blas A; Rodríguez-Blas T; Platas-Iglesias C Understanding Stability Trends along the Lanthanide Series. Chem. - Eur. J 2014, 20, 3974–3981. [PubMed: 24577810]

(43). Ferreirós-Martínez R; Esteban-Gómez D; Tóth É; de Blas A; Platas-Iglesias C; Rodríguez-Blas T Macrocyclic Receptor Showing Extremely High Sr(II)/Ca(II) and Pb(II)/Ca(II) Selectivities with Potential Application in Chelation Treatment of Metal Intoxication. Inorg. Chem 2011, 50, 3772–3784. [PubMed: 21413756]

(44). Thiele NA; MacMillan SN; Wilson JJ Rapid Dissolution of BaSO4 by Macropa, an 18-Membered Macrocycle with High Affinity for Ba^{2+}. J. Am. Chem. Soc 2018, 140, 17071–17078. [PubMed: 30485079]

(45). Fiszbein DJ; Brown V; Thiele NA; Woods JJ; Wharton L; MacMillan SN; Radchenko V; Ramogida CF; Wilson JJ Tuning the Kinetic Inertness of Bi^{3+} Complexes: The Impact of Donor Atoms on Diaza-18-Crown-6 Ligands as Chelators for ^{213}Bi Targeted Alpha Therapy. Inorg. Chem 2021, 60, 9199–9211. [PubMed: 34102841]

(46). McDevitt MR; Ma D; Simon J; Frank RK; Scheinberg DA Design and Synthesis of ^{225}Ac Radioimmunopharmaceuticals. Appl. Radiat. Isot 2002, 57, 841–847. [PubMed: 12406626]

(47). Maguire WF; McDevitt MR; Smith-Jones PM; Scheinberg DA Efficient 1-Step Radiolabeling of Monoclonal Antibodies to High Specific Activity with 225 Ac for α-Particle Radioimmunotherapy of Cancer. J. Nucl. Med 2014, 55, 1492–1498. [PubMed: 24982438]

(48). Deblonde GJ-P; Zavarin M; Kersting AB The Coordination Properties and Ionic Radius of Actinium: A 120-Year-Old Enigma. Coord. Chem. Rev 2021, 446, 214130.

(49). Aluicio-Sarduy E; Hernandez R; Olson AP; Barnhart TE; Cai W; Ellison PA; Engle JW Production and *in vivo* PET/CT Imaging of the Theranostic Pair $^{132/135}$La. Sci. Rep 2019, 9, 10658. [PubMed: 31337833]

(50). Aluicio-Sarduy E; Thiele NA; Martin KE; Vaughn BA; Devaraj J; Olson AP; Barnhart TE; Wilson JJ; Boros E; Engle JW Establishing Radiolanthanum Chemistry for Targeted Nuclear Medicine Applications. Chem. - Eur. J 2020, 26, 1238–1242. [PubMed: 31743504]

(51). Kluetz PG; Pierce W; Maher VE; Zhang H; Tang S; Song P; Liu Q; Haber MT; Leutzinger EE; Al-Hakim A; Chen W; Palmby T; Alebachew E; Sridhara R; Ibrahim A; Justice R; Pazdur R Radium Ra 223 Dichloride Injection: U.S. Food and Drug Administration Drug Approval Summary. Clin. Cancer Res 2014, 20, 9–14. [PubMed: 24190979]

(52). Reissig F; Bauer D; Ullrich M; Kreller M; Pietzsch J; Mamat C; Kopka K; Pietzsch H-J; Walther M Recent Insights in Barium-131 as a Diagnostic Match for Radium-223: Cyclotron Production, Separation, Radiolabeling, and Imaging. Pharmaceuticals 2020, 13, 272.

(53). Lewington VJ Bone-Seeking Radionuclides For Therapy. J. Nucl. Med 2005, 46, 38S–47S. [PubMed: 15653650]

(54). Shimoni-Livny L; Glusker JP; Bock CW Lone Pair Functionality in Divalent Lead Compounds. Inorg. Chem 1998, 37, 1853–1867.

(55). Pujales-Paradela R; Rodríguez-Rodríguez A; Gayoso-Padula A; Brandariz I; Valencia L; Esteban-Gómez D; Platas-Iglesias C On the Consequences of the Stereochemical Activity of the Bi(iii) $6s^2$ Lone Pair in Cyclen-Based Complexes. The [Bi(DO3A)] Case. Dalton Trans. 2018, 47, 13830–13842. [PubMed: 30230496]

(56). Baba K; Nagata K; Yajima T; Yoshimura T Synthesis, Structures, and Equilibrium Reactions of La(III) and Ba(II) Complexes with Pyridine Phosphonate Pendant Arms on a Diaza-18-crown-6 Ether. Bull. Chem. Soc. Jpn 2022, doi: 10.1246/bcsj.20210414.

(57). Panchenko PA; Zubenko AD; Chernikova EY; Fedorov YV; Pashanova AV; Karnoukhova VA; Fedyanin IV; Fedorova OA Synthesis, Structure and Metal Ion Coordination of Novel Benzodiazamacrocyclic Ligands Bearing Pyridyl and Picolinate Pendant Side-Arms. New J. Chem 2019, 43, 15072–15086.

(58). Zeglis BM; Lewis JS A Practical Guide to the Construction of Radiometallated Bioconjugates for Positron Emission Tomography. Dalton Trans. 2011, 40, 6168–6195. [PubMed: 21442098]

(59). Lattuada L; Barge A; Cravotto G; Giovenzana GB; Tei L The Synthesis and Application of Polyamino Polycarboxylic Bifunctional Chelating Agents. Chem. Soc. Rev 2011, 40, 3019–3049. [PubMed: 21384039]

(60). Kwon H; Son S-H; Byun Y Prostate-Specific Membrane Antigen (PSMA)-Targeted Radionuclide Probes for Imaging and Therapy of Prostate Cancer. Asian J. Org. Chem 2019, 8, 1588–1600.

(61). Dumelin CE; Trüssel S; Buller F; Trachsel E; Bootz F; Zhang Y; Mannocci L; Beck SC; Drumea-Mirancea M; Seeliger MW; Baltes C; Müggler T; Kranz F; Rudin M; Melkko S; Scheuermann J; Neri D A Portable Albumin Binder from a DNA-Encoded Chemical Library. Angew. Chem., Int. Ed 2008, 47, 3196–3201.

(62). Kelly JM; Amor-Coarasa A; Ponnala S; Nikolopoulou A; Williams C; Thiele NA; Schlyer D; Wilson JJ; DiMagno SG; Babich JW A Single Dose of ^{225}Ac-RPS-074 Induces a Complete Tumor Response in an LNCaP Xenograft Model. J. Nucl. Med 2019, 60, 649–655. [PubMed: 30413660]

(63). Bell MM; Gutsche NT; King AP; Baidoo KE; Kelada OJ; Choyke PL; Escorcia FE Glypican-3-Targeted Alpha Particle Therapy for Hepatocellular Carcinoma. Molecules 2020, 26, 4.

(64). Ishiguro T; Sugimoto M; Kinoshita Y; Miyazaki Y; Nakano K; Tsunoda H; Sugo I; Ohizumi I; Aburatani H; Hamakubo T; Kodama T; Tsuchiya M; Yamada-Okabe H Anti–Glypican 3 Antibody as a Potential Antitumor Agent for Human Liver Cancer. Cancer Res. 2008, 68, 9832–9838. [PubMed: 19047163]

(65). Reissig F; Bauer D; Zarschler K; Novy Z; Bendova K; Ludik M-C; Kopka K; Pietzsch H-J; Petrik M; Mamat C Towards Targeted Alpha Therapy with Actinium-225: Chelators for Mild Condition Radiolabeling and Targeting PSMA—A Proof of Concept Study. Cancers 2021, 13, 1974. [PubMed: 33923965]

(66). Haldón E; Nicasio MC; Pérez PJ Copper-Catalysed Azide–Alkyne Cycloadditions (CuAAC): An Update. Org. Biomol. Chem 2015, 13, 9528–9550. [PubMed: 26284434]

(67). Hu A; Wilson JJ Unpublished Result.

(68). Li L; Jaraquemada-Peláez M de G; Kuo H-T; Merkens H; Choudhary N; Gitschtaler K; Jermilova U; Colpo N; Uribe-Munoz C; Radchenko V; Schaffer P; Lin K-S; Bénard F; Orvig C Functionally Versatile and Highly Stable Chelator for ^{111}In and ^{177}Lu: Proof-of-Principle Prostate-Specific Membrane Antigen Targeting. Bioconjugate Chem. 2019, 30, 1539–1553.

(69). Hu A; Keresztes I; MacMillan SN; Yang Y; Ding E; Zipfel WR; DiStasio RA Jr.; Babich JW; Wilson JJ Oxyaapa: A Picolinate-Based Ligand with Five Oxygen Donors that Strongly Chelates Lanthanides. Inorg. Chem 2020, 59, 5116–5132. [PubMed: 32216281]

(70). Hu A; Brown V; MacMillan SN; Radchenko V; Yang H; Wharton L; Ramogida CF; Wilson JJ Chelating the Alpha Therapy Radionuclides $^{225}Ac^{3+}$ and $^{213}Bi^{3+}$ with 18-Membered Macrocyclic Ligands Macrodipa and Py-Macrodipa. Inorg. Chem 2022, 61, 801–806. [PubMed: 34965102]

KEY REFERENCES

- Thiele, N. A.; Brown, V.; Kelly, J. M.; Amor-Coarasa, A.; Jermilova, U.; MacMillan, S. N.; Nikolopoulou, A.; Ponnala, S.; Ramogida, C. F.; Robertson, A. K. H.; Rodríguez-Rodríguez, C.; Schaffer, P.; Williams, C., Jr.; Babich, J. W.; Radchenko, V.; Wilson, J. J. An Eighteen-Membered Macrocyclic Ligand for Actinium-225 Targeted Alpha Therapy. *Angew. Chem., Int. Ed.* **2017**, *56*, 14712–14717.[1] *This study reports the effectiveness of the chelator macropa in binding the α-emitter* $^{225}Ac^{3+}$. *A bifunctional derivative macropa-NCS was developed, and a macropa-based bioconjugate RPS-070 was constructed. In vivo studies revealed selective uptake of its* ^{225}*Ac–RPS-070 complex in a mouse xenograft model of prostate cancer.*

- Hu, A.; MacMillan, S. N.; Wilson, J. J. Macrocyclic Ligands with an Unprecedented Size-Selectivity Pattern for the Lanthanide Ions. *J. Am. Chem. Soc.* **2020**, *142*, 13500–13506.[2] *This work establishes the concept of "dual size selectivity" with two chelators, macrodipa and macrotripa. They show good affinities to both the large and small lanthanide ions by toggling between two distinct conformations.*

- Abou, D. S.; Thiele, N. A.; Gutsche, N. T.; Villmer, A.; Zhang, H.; Woods, J. J.; Baidoo, K. E.; Escorcia, F. E.; Wilson, J. J.; Thorek, D. L. J. Towards the Stable Chelation of Radium for Biomedical Applications with an 18-Membered Macrocyclic Ligand. *Chem. Sci.* **2021**, *12*, 3733–3742.[3] *This work validates macropa as an efffective chelator for* $^{223}Ra^{2+}$. *Moreover, it reports the in vivo investigation of a* $^{223}Ra^{2+}$ *radiopharmacetical.*

- Hu, A.; Aluicio-Sarduy, E.; Brown, V.; MacMillan, S. N.; Becker, K. V; Barnhart, T. E.; Radchenko, V.; Ramogida, C. F.; Engle, J. W.; Wilson, J. J. Py-Macrodipa: A Janus Chelator Capable of Binding Medicinally Relevant Rare-Earth Radiometals of Disparate Sizes. *J. Am. Chem. Soc.* **2021**, *143*, 10429–10440.[4] *A demonstration of the development of the dual-size-selective chelator py-macrodipa, and its application in nuclear medicine is presented. Py-macrodipa efficiently forms stable complexes with both large* $^{135}La^{3+}$ *and small* $^{44}Sc^{3+}$.

Figure 1.

Rare-earth elements. Spheres are scaled by the 6-coordinate ionic radius[28] of their trivalent cations (Ln^{3+}). Their atomic numbers are labeled above.

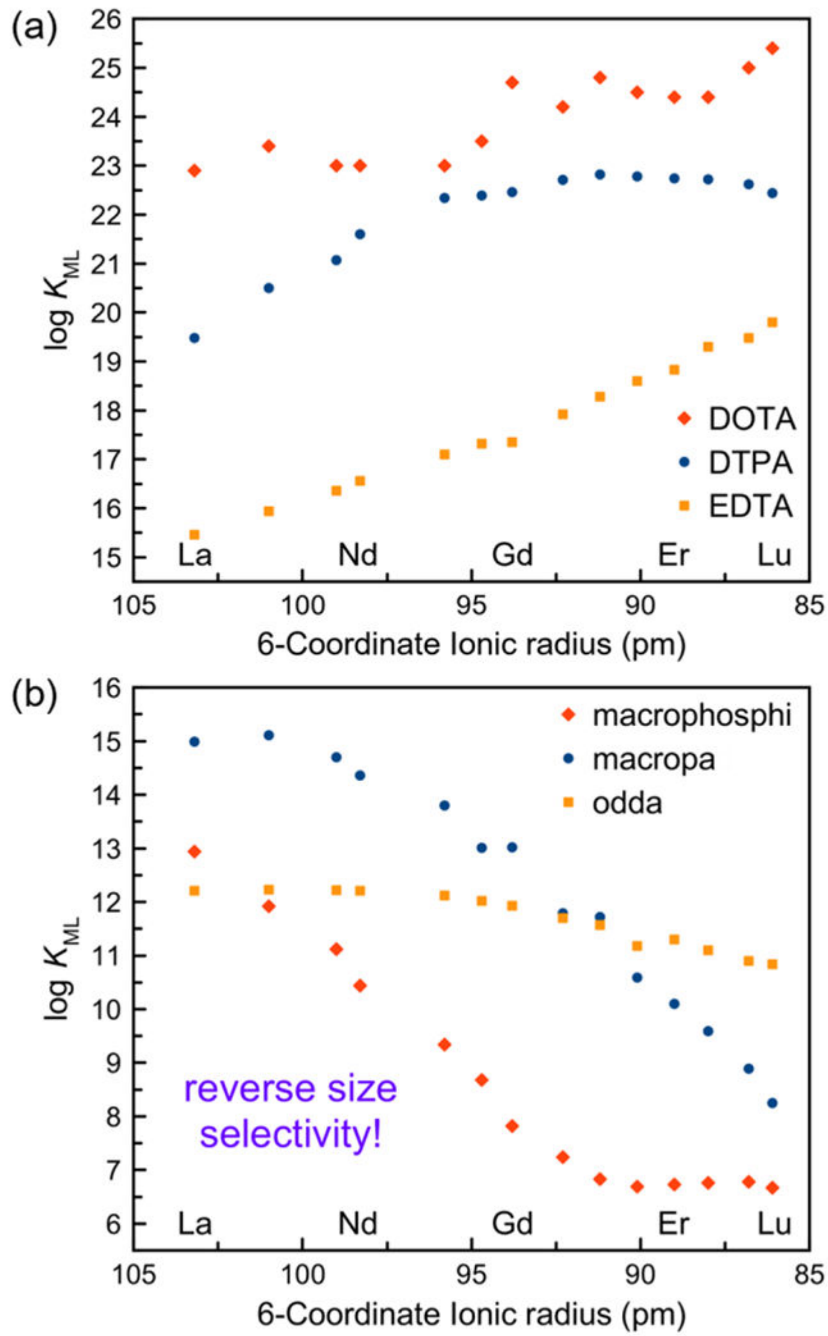

Figure 2.

K_{ML} values of Ln^{3+} complexes formed with (a) DOTA, DTPA, EDTA and (b) odda, macropa, macrophosphi plotted versus ionic radii. Data obtained from refs 33–39.

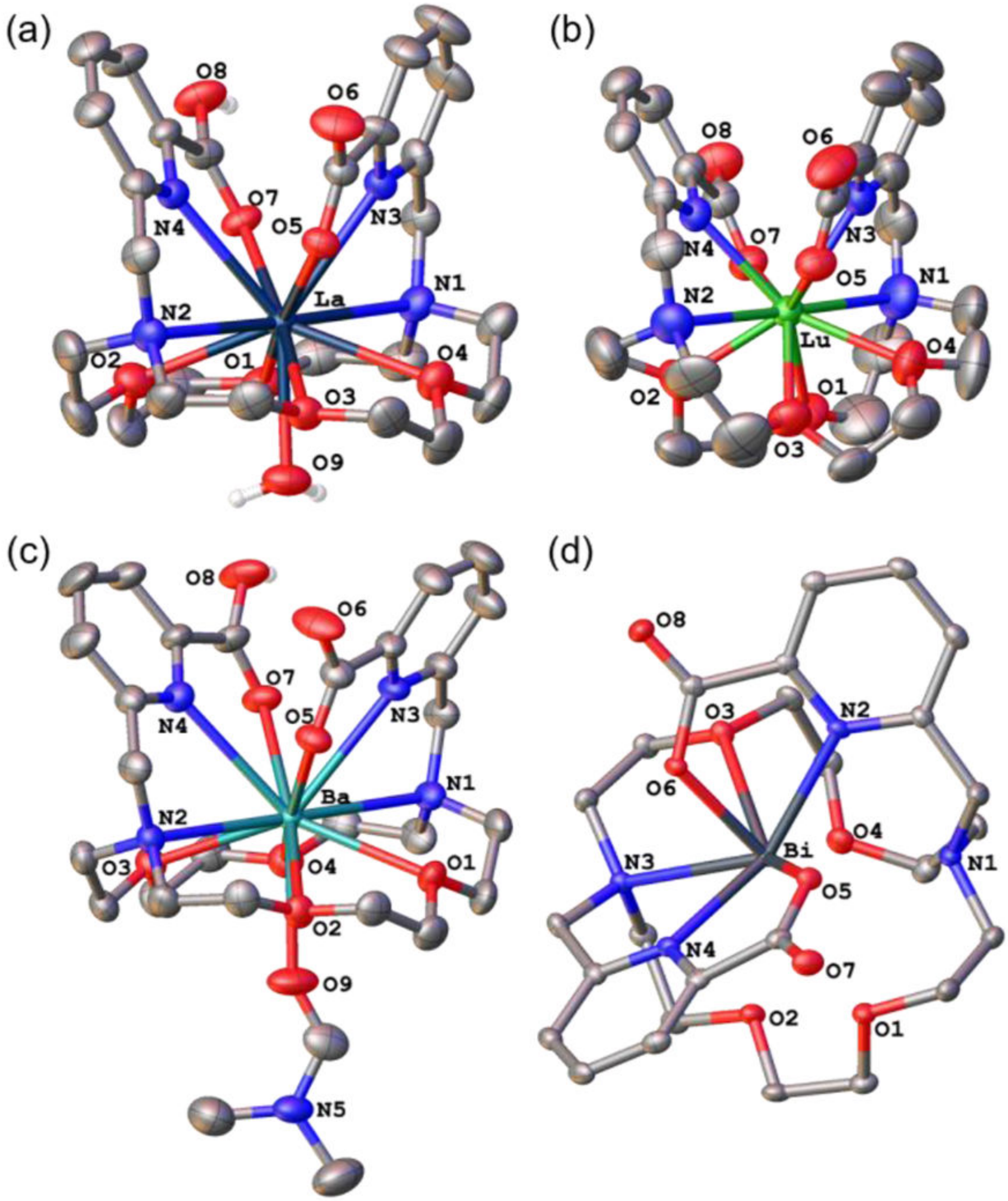

Figure 3.

Crystal structures of (a) $[La(Hmacropa)(OH_2)]^{2+}$, (b) $[Lu(macropa)]^{+}$, (c) $[Ba(Hmacropa)(DMF)]^{+}$, and (d) $[Bi(macropa)]^{+}$. Counterions, nonacidic hydrogen atoms, and outer-sphere solvent molecules are omitted for clarity. Crystallographic data are from refs 1,44,45.

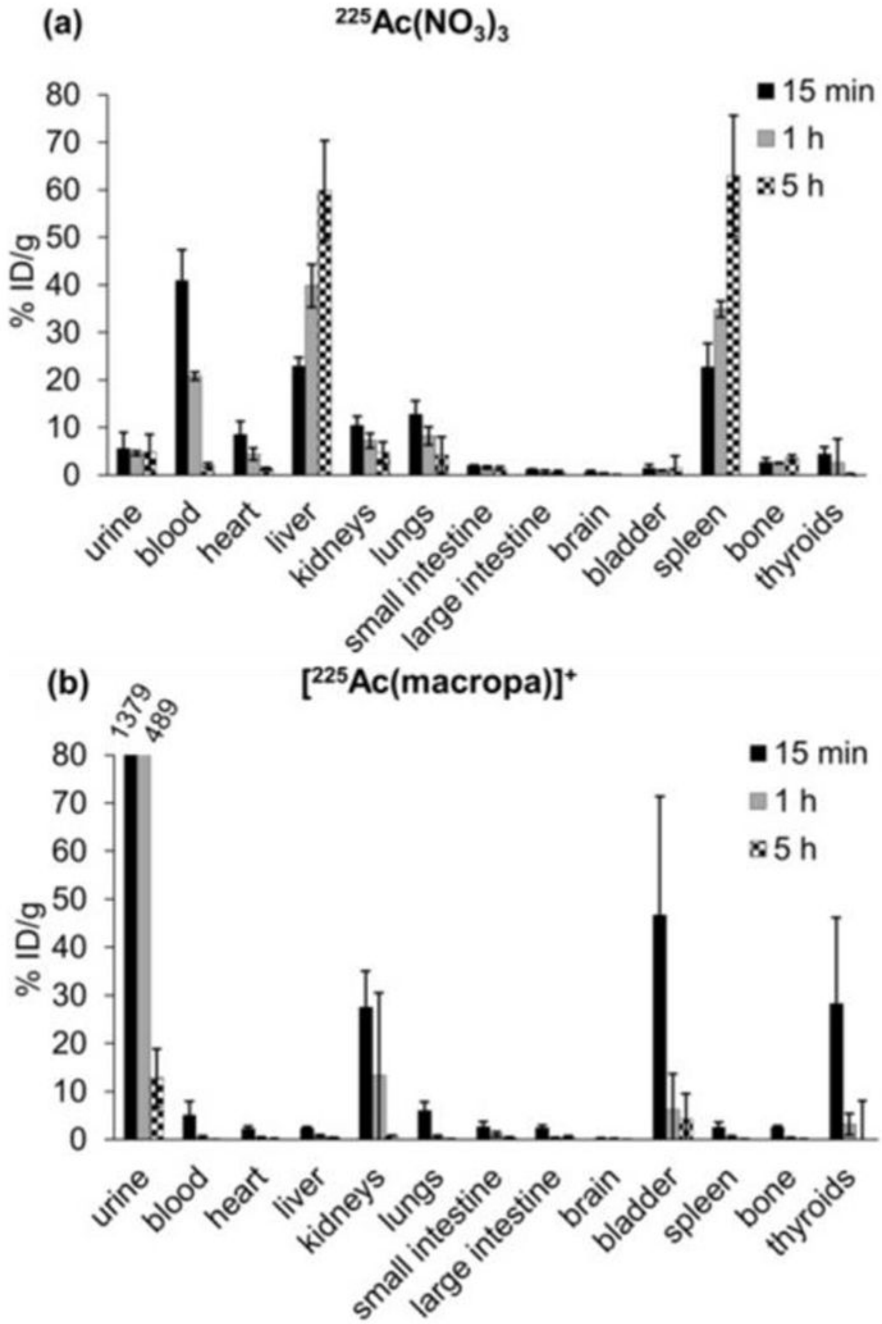

Figure 4.

Biodistribution of (a) [^{225}Ac]Ac(NO$_3$)$_3$ and (b) [^{225}Ac][Ac(macropa)]$^+$ following intravenous injection in adult C57BL/6 mice. The numbers written over "urine" are their measured %ID·g^{-1}, which are off-scale compared to other organs. Adapted with permission from ref 1. Copyright 2017 Wiley-VCH Verlag GmbH &Co. KGaA, Weinheim.

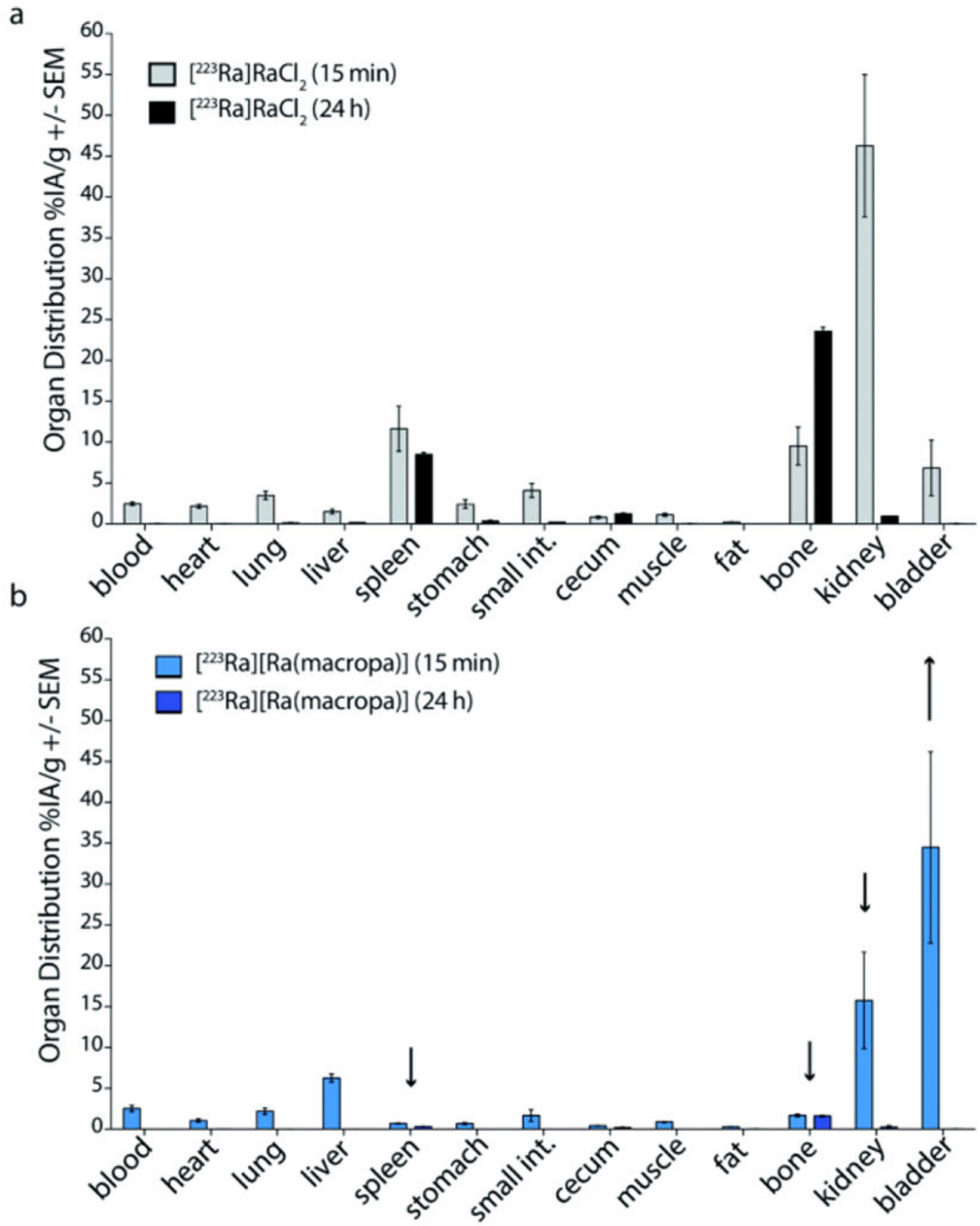

Figure 5.

Biodistribution of (a) [^{223}Ra]RaCl$_2$ and (b) [^{223}Ra][Ra(macropa)] in healthy, skeletally mature mice sacrificed at 15 min and 24 h post injection. Adapted with permission from ref 3. Copyright 2021 Royal Society of Chemistry.

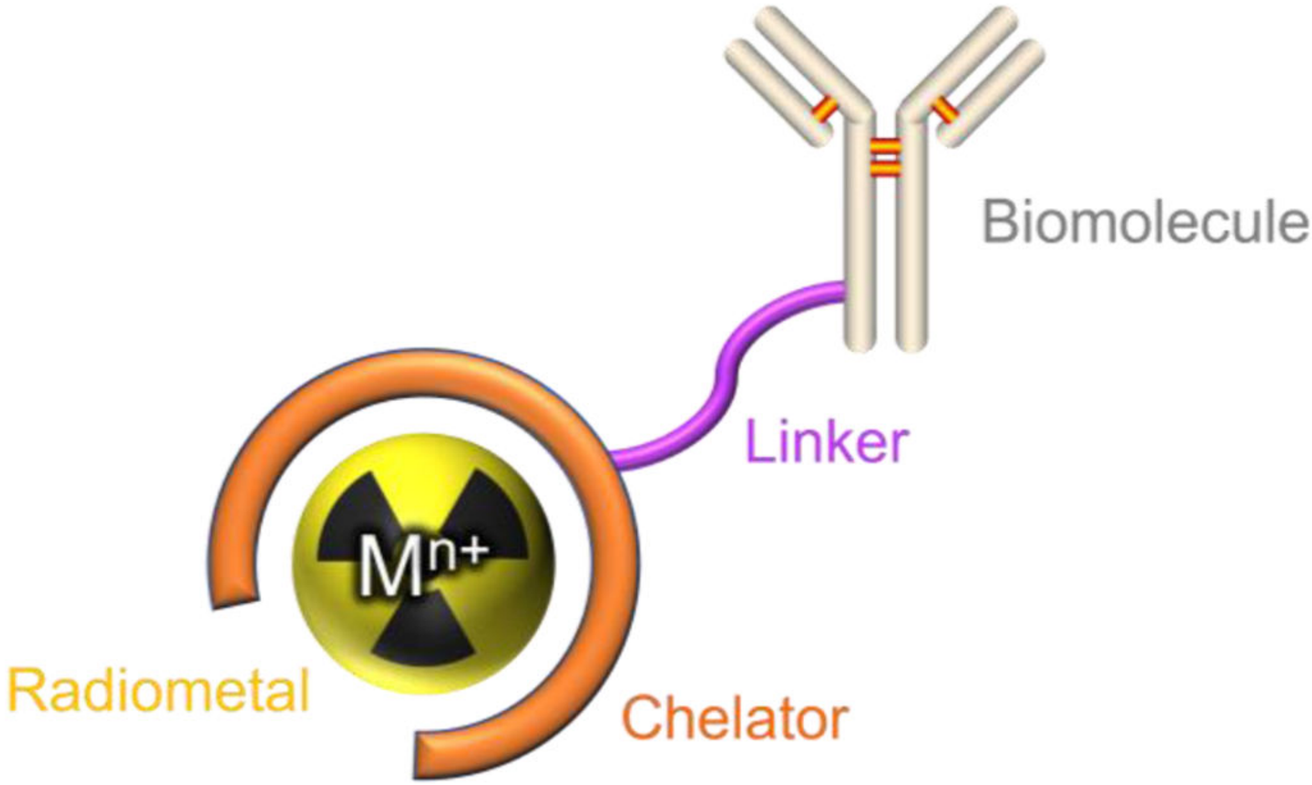

Figure 6.
Schematic representation of a bioconjugate used for nuclear medicine.

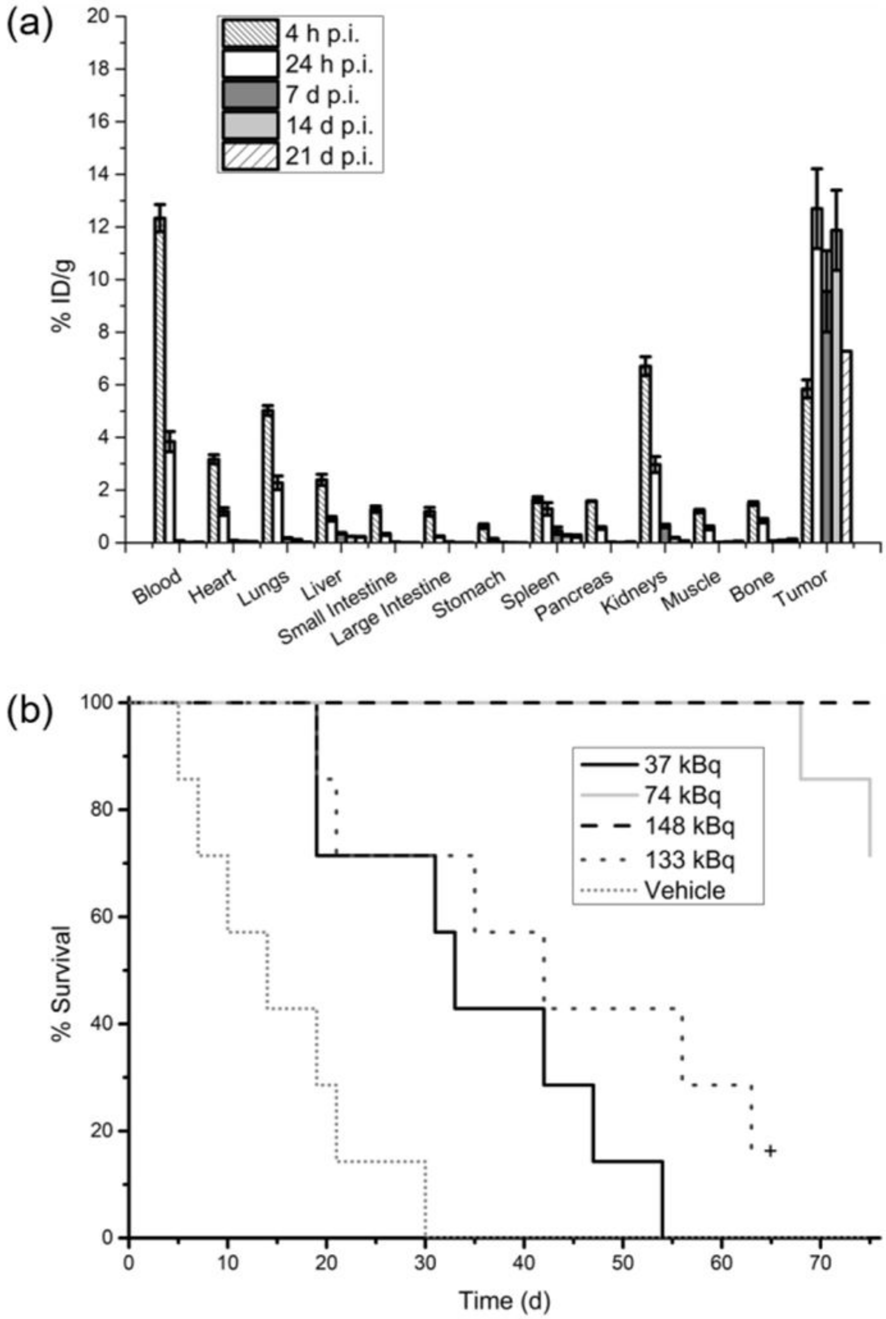

Figure 7.

(a) Biodistribution of ^{225}Ac–RPS-074 following intravenous injection in male BALB/c *nu/nu* mice bearing LNCaP xenograft tumors. (b) Kaplan–Meier plot comparing survival of male BALB/c *nu/nu* mice bearing LNCaP xenograft tumors treated with different doses of ^{225}Ac–RPS-074. Reproduced with permission from ref [62]. Copyright 2019 Society of Nuclear Medicine and Molecular Imaging.

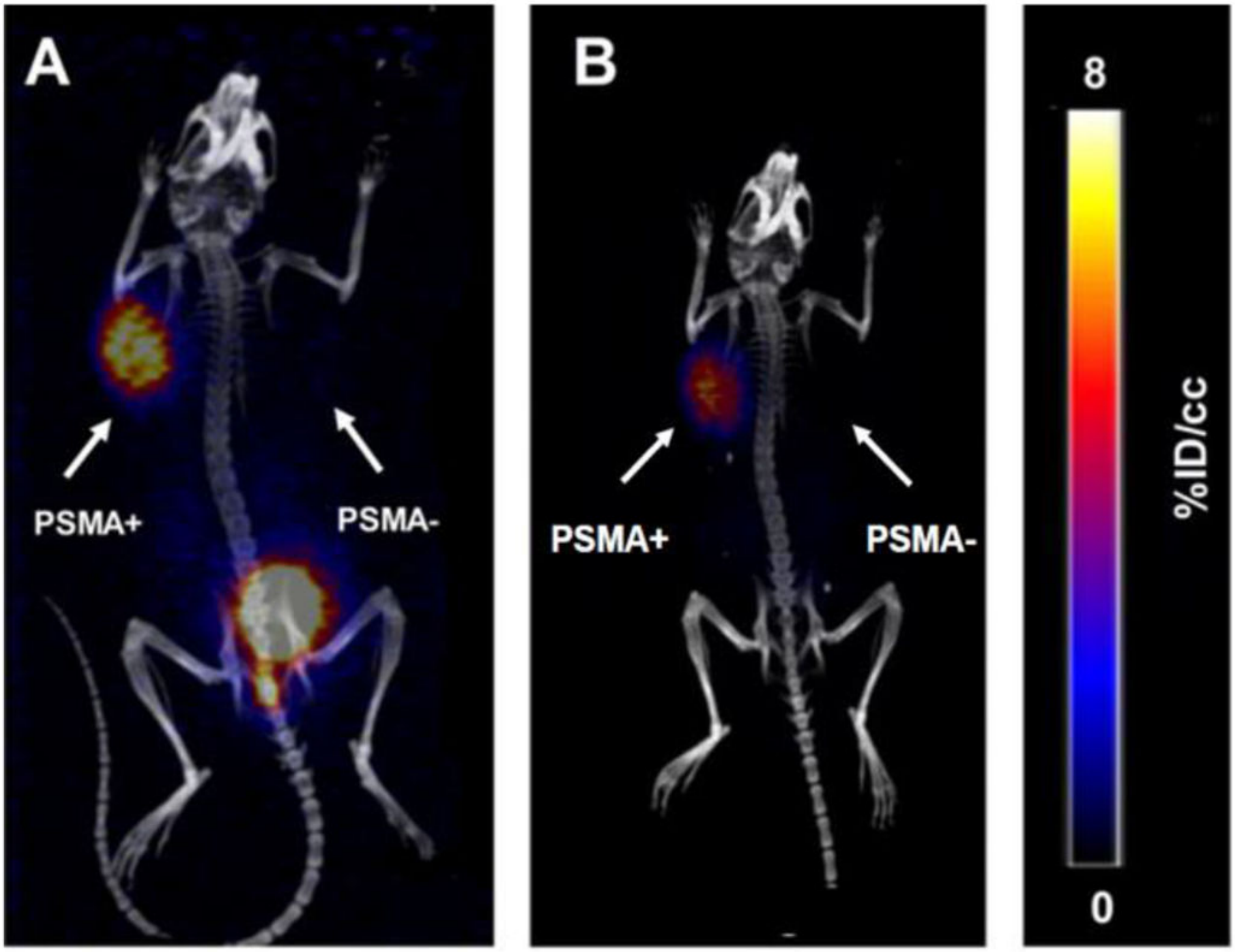

Figure 8.
Representative PET/CT images of PC3-PIP/flu tumor bearing mice (A) 1 h and (B) 4 h after injection of $^{132/135}$La–macropa-DUPA. Adapted with permission from ref [50]. Copyright 2019 Wiley-VCH Verlag GmbH & Co. KGaA, Weinheim.

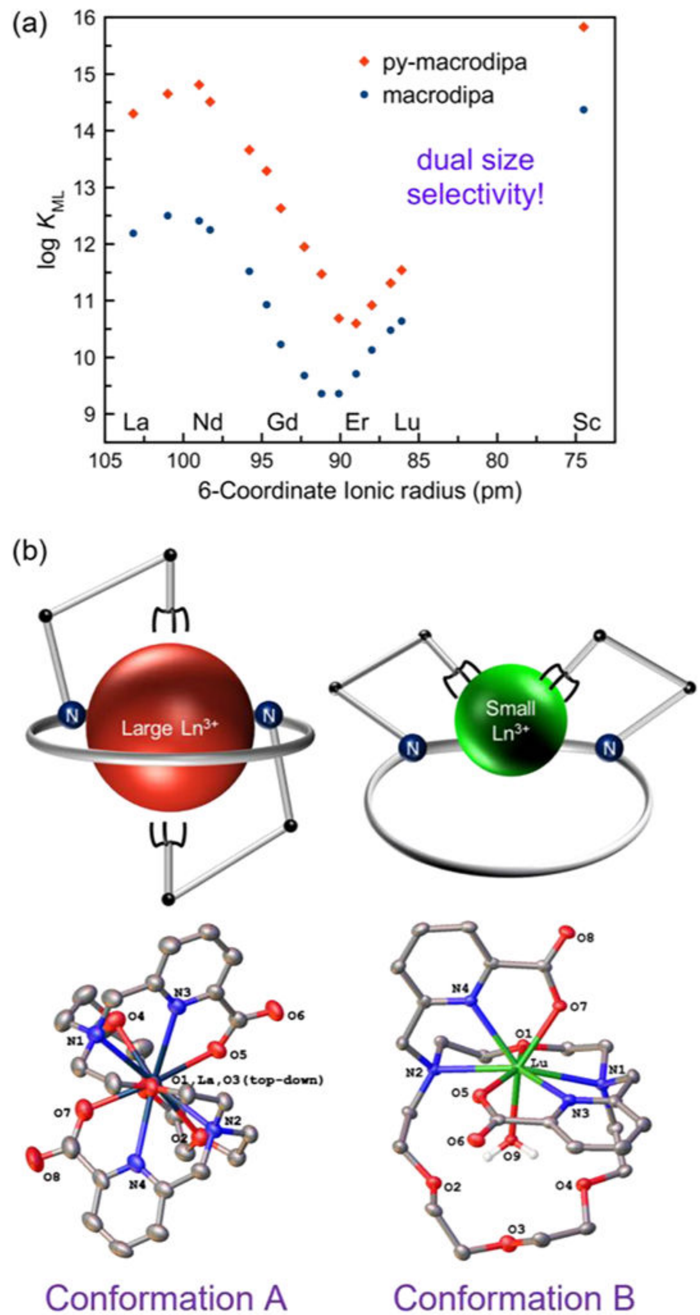

Figure 9.

(a) K_{ML} values of Ln^{3+} complexes formed with macrodipa and py-macrodipa plotted versus ionic radii. (b) Illustration of the conformational toggle in macrodipa that occurs during complexation with large and small Ln^{3+} ions, as verified by representative crystal structures of $[La(macrodipa)]^+$ and $[Lu(macrodipa)(OH_2)]^+$. Data adapted from refs 2,4.

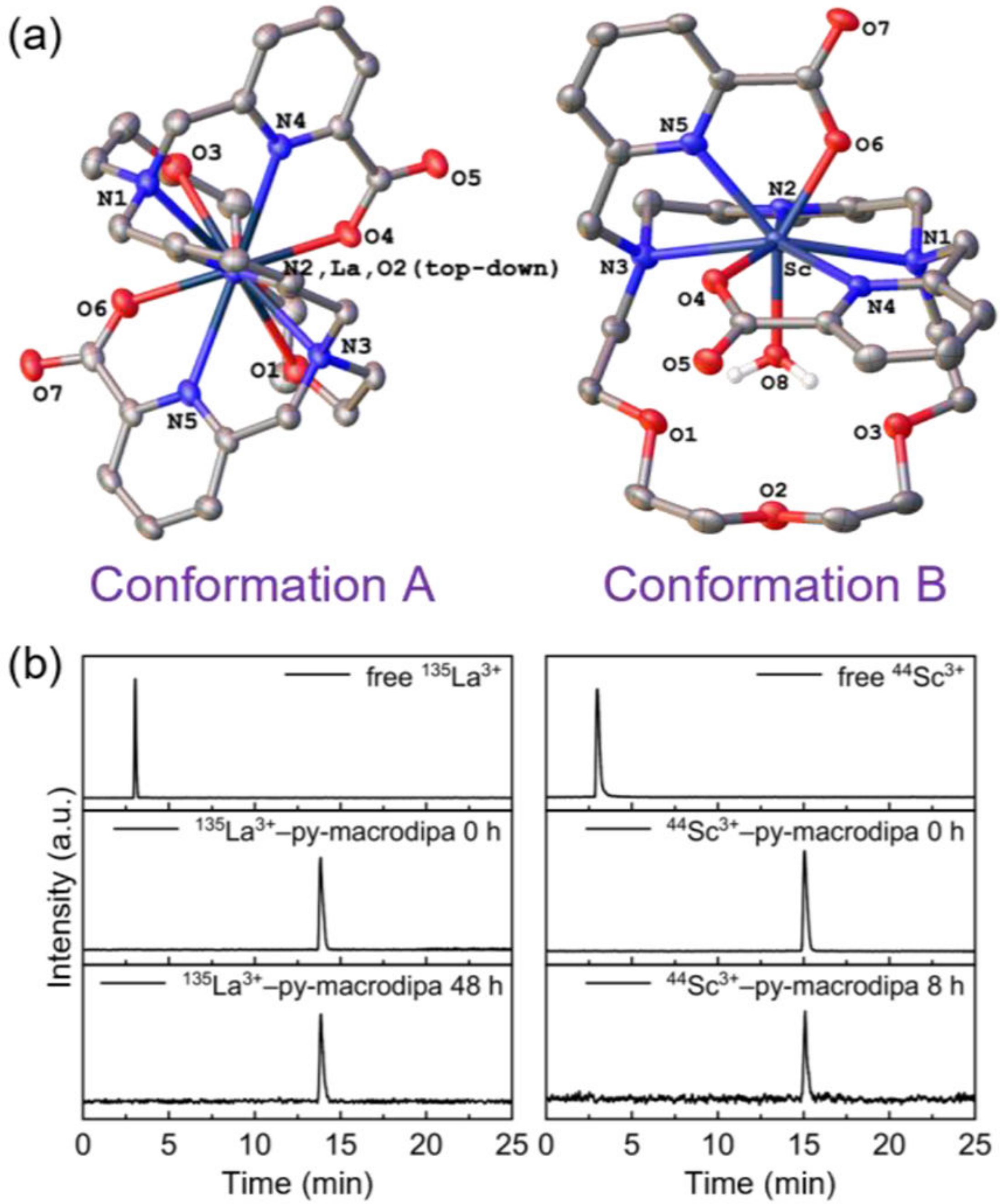

Figure 10.

(a) Crystal structures of $[La(py\text{-}macrodipa)]^+$ and $[Sc(py\text{-}macrodipa)(OH_2)]^+$, which represent Conformations A and B, respectively. (b) Human serum challenge assay for $[^{135}La][La(py\text{-}macrodipa)]^+$ and $[^{44}Sc][Sc(py\text{-}macrodipa)(OH_2)]^+$ complexes, monitored by radio-HPLC. Data adapted from ref 4.

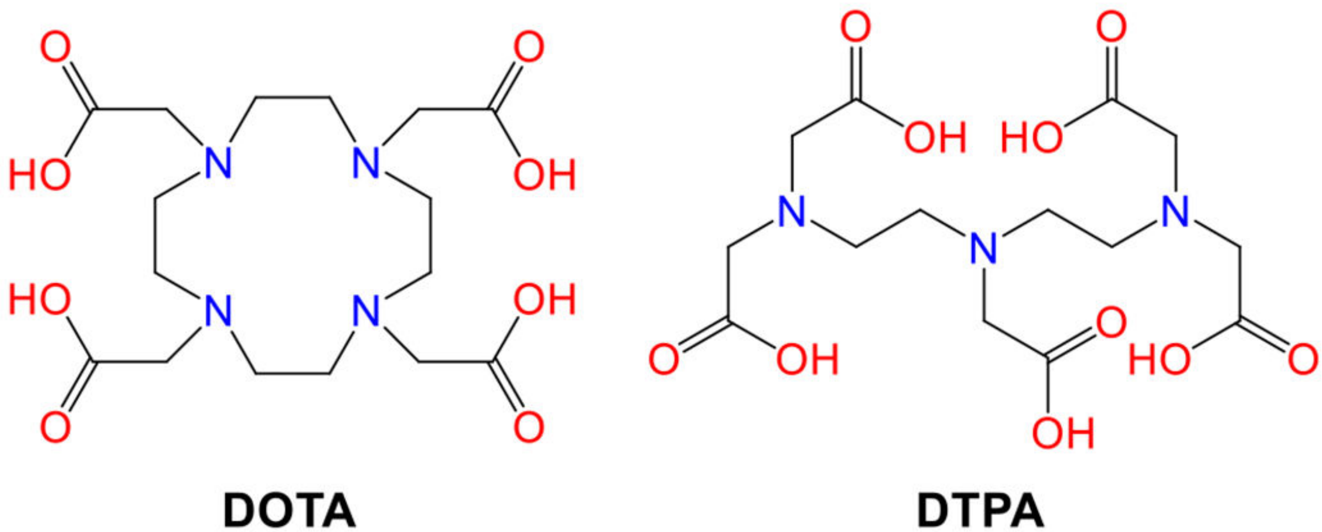

Chart 1.
Structures of DOTA and DTPA.

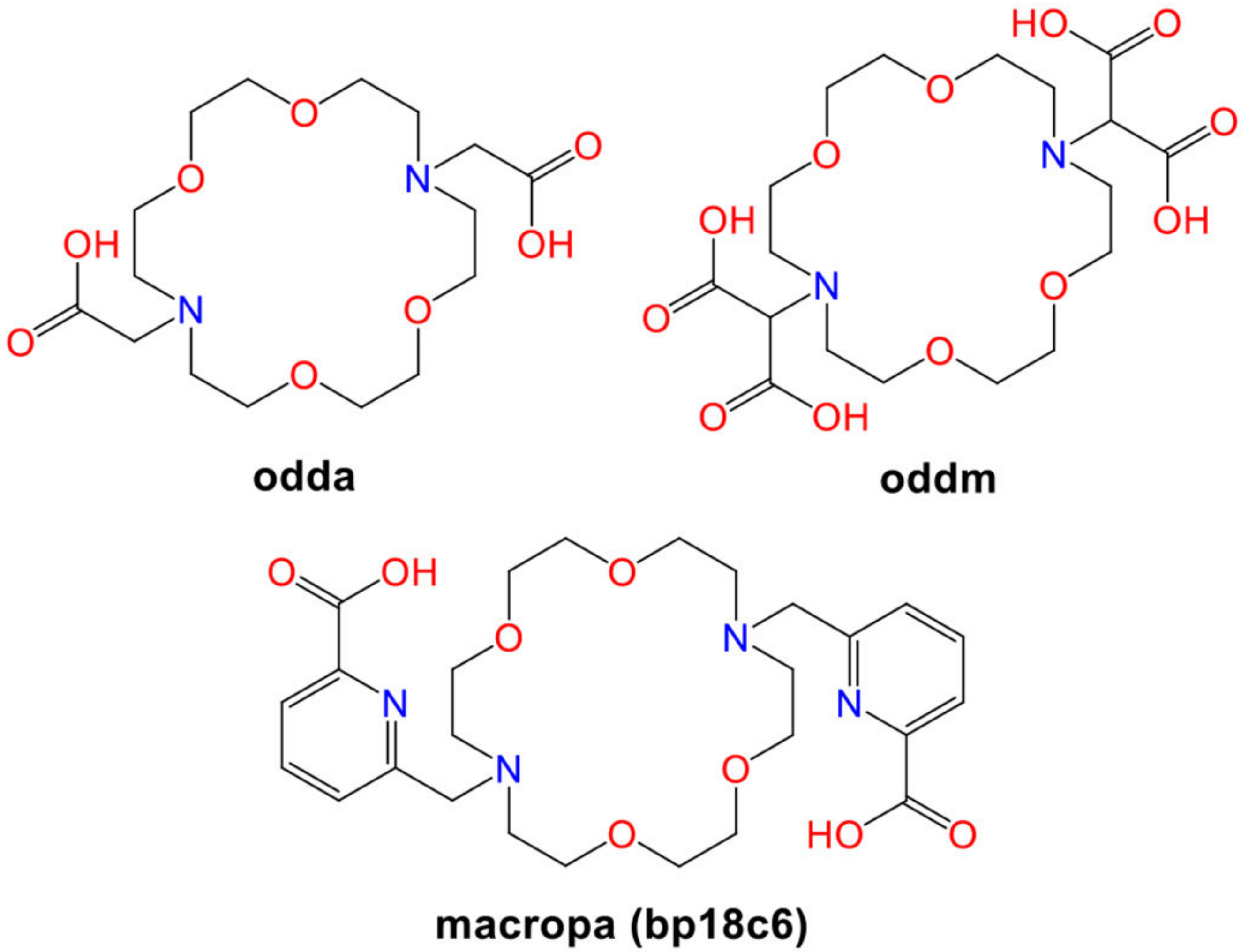

Chart 2.
Structures of odda, oddm, and macropa.

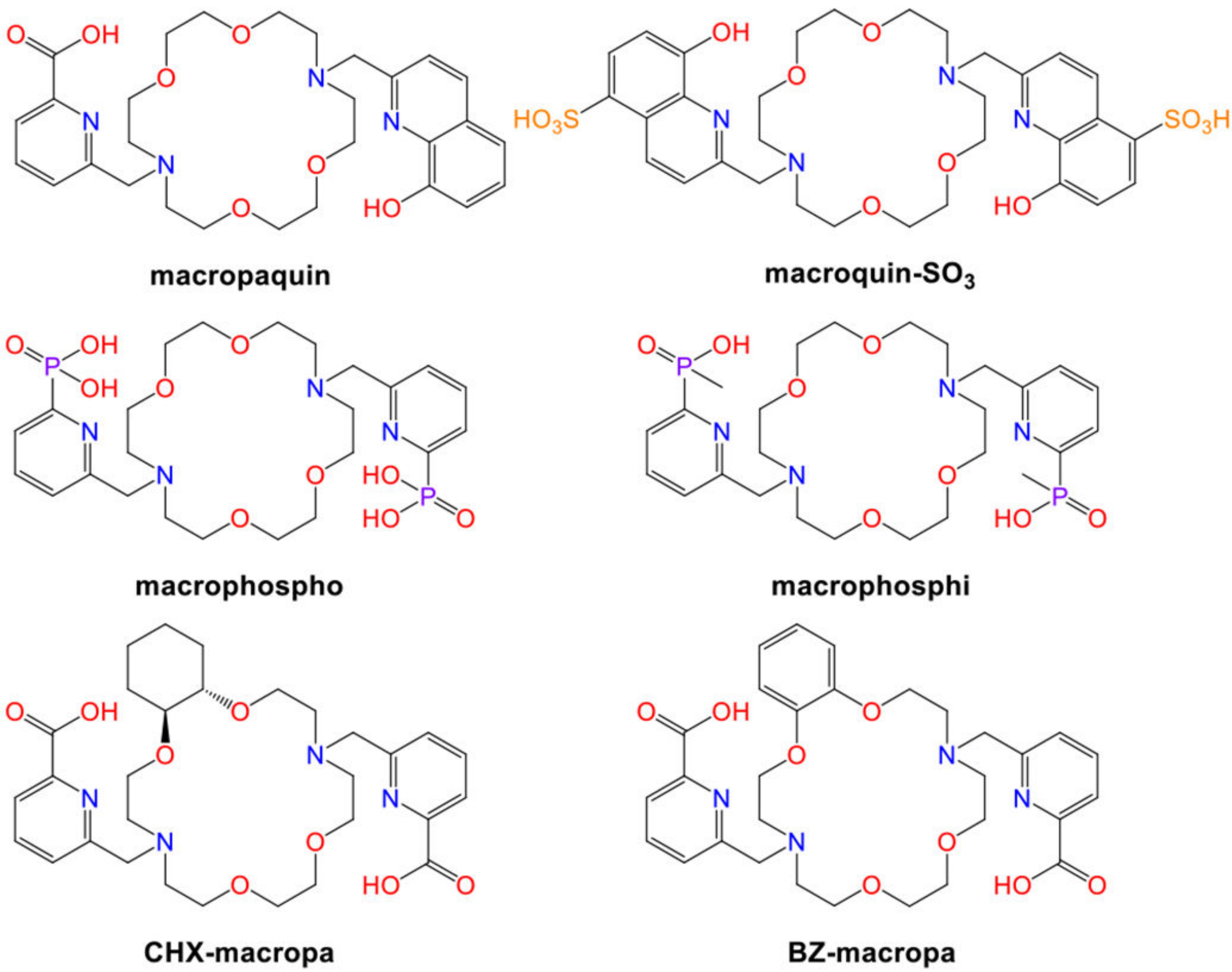

Chart 3.

Structures of Macropa Derivatives Discussed in this Manuscript.

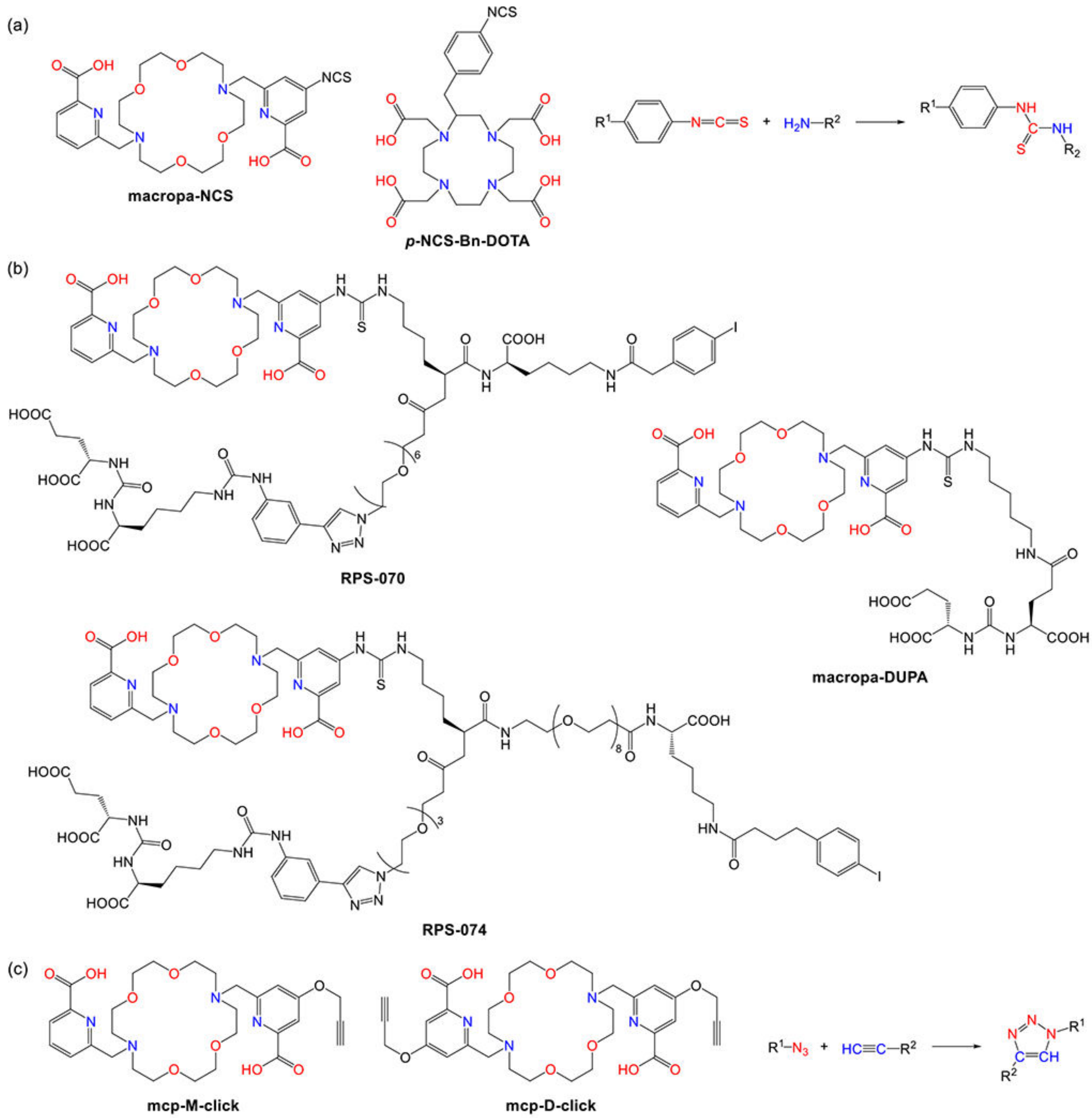

Chart 4.
(a) Structures of Bifunctional Chelators macropa-NCS, *p*-NCS-Bn-DOTA, and their Corresponding Conjugation Reaction. (b) Structures of Bioconjugates RPS-070, RPS-074, and macropa-DUPA. (c) Structures of Bifunctional Chelators mcp-M-click, mcp-D-click, and their Corresponding Conjugation Reaction.

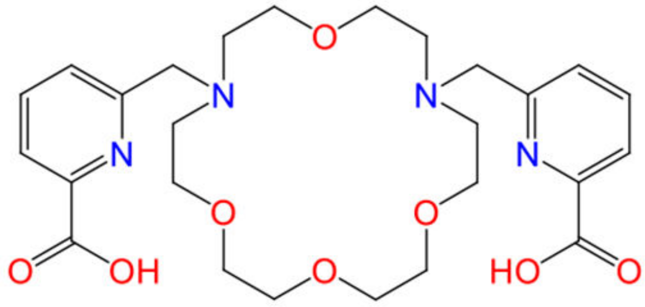

macrodipa

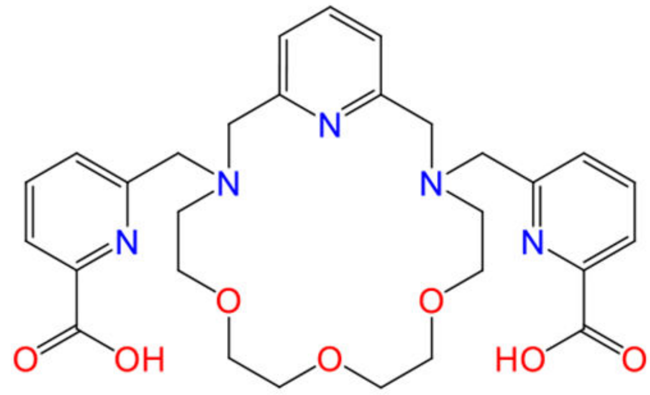

py-macrodipa

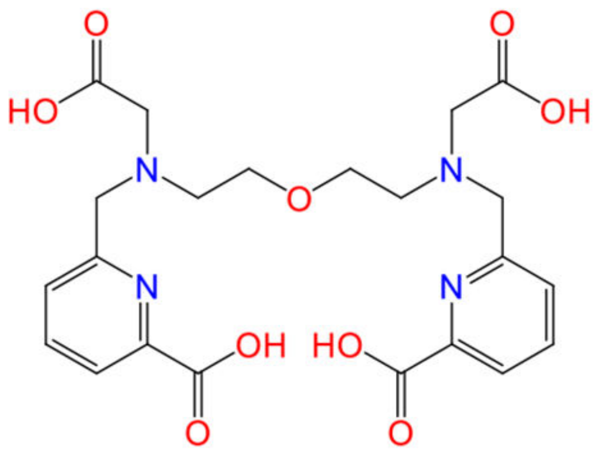

Oxyaapa

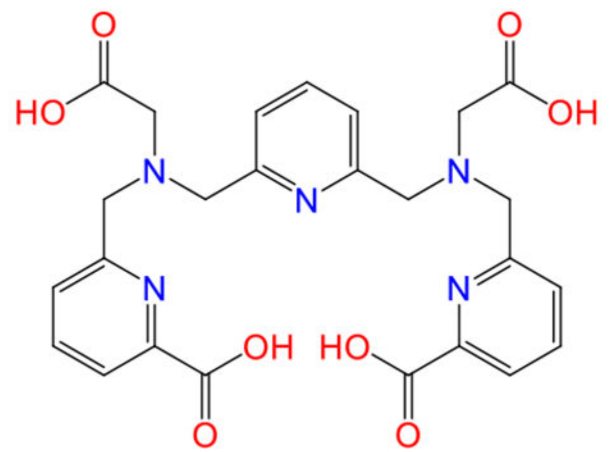

pypa

Chart 5.
Structures of macrodipa, py-macrodipa, Oxyaapa, and pypa.

Table 1.

Large Radiometals Relevant to Nuclear Medicine.

Radiometal	Half-life	Major decay mode	Application	Ref
^{132}La	4.59 h	β^+	PET	13
^{134}La	6.45 min	β^+	PET	14
^{135}La	18.9 h	electron capture	Auger electron therapy	15
^{134}Ce	3.16 d	electron capture	PET[a]	14
^{225}Ac	9.9 d	α	*α* therapy	16
^{212}Bi	60.6 min	β^-, α	*α* therapy[b]	17
^{213}Bi	45.6 min	β^-	*α* therapy[b]	17
^{131}Ba	11.5 d	electron capture	SPECT	18
^{223}Ra	11.4 d	α	*α* therapy	19
^{212}Pb	10.6 h	β^-	*α* therapy[b]	20
^{227}Th	18.7 d	α	*α* therapy	21
^{230}U	20.8 d	α	*α* therapy	22

[a] ^{134}Ce is regarded as a PET imager due to its positron-emitting daughter ^{134}La, despite its decay mode (electron capture).

[b] These radionuclides are categorized as α therapy candidates due to their α-emitting daughters, despite their major decay modes (β^-).